



33 **Abstract**

34 The 2010 international thermodynamic equation of seawater, TEOS-10, defined the
35 enthalpy and entropy of seawater, thus enabling the global ocean heat content to be
36 calculated as the volume integral of the product of in situ density, ρ , and potential
37 enthalpy, h^0 (with reference sea pressure of 0 dbar). In terms of Conservative
38 Temperature, Θ , ocean heat content is the volume integral of $\rho c_p^0 \Theta$, where c_p^0 is a
39 constant “isobaric heat capacity”.

40 However, several ocean models in CMIP6 (as well as all of those in previous
41 Coupled Model Intercomparison Project phases, such as CMIP5) have not been
42 converted from EOS-80 (Equation of State - 1980) to TEOS-10, so the question arises of
43 how the salinity and temperature variables in these models should be interpreted. In
44 this article we address how heat content, surface heat fluxes and the meridional heat
45 transport are best calculated in these models, and also how these quantities should be
46 compared with the corresponding quantities calculated from observations. We
47 conclude that even though a model uses the EOS-80 equation of state which expects
48 potential temperature as its input temperature, the most appropriate interpretation of
49 the model’s temperature variable is actually Conservative Temperature. This
50 interpretation is needed to ensure that the air-sea heat flux that leaves/arrives-in the
51 atmosphere is the same as that which arrives-in/leaves the ocean.

52 We also show that the salinity variable carried by TEOS-10 based models is
53 Preformed Salinity, while the prognostic salinity of EOS-80 based models is also
54 proportional to Preformed Salinity. These interpretations of the salinity and
55 temperature variables in ocean models are an update on the comprehensive Griffies et
56 al (2016) paper that discusses the interpretation of many aspects of coupled model
57 runs.

58



59 1. Introduction

60 Numerical ocean models simulate the real ocean by calculating the acceleration
61 of fluid parcels in response to various forces, some of which are related to spatially-
62 varying density fields, as well as solving transport equations for the two tracers on
63 which density depends, namely heat content (“temperature”) and dissolved matter
64 (“salinity”). For computational reasons it is useful for the numerical schemes involved
65 to be conservative, meaning that the overall amount of heat and salt in the ocean
66 changes only due to fluxes across the ocean’s boundaries. This is guaranteed even for
67 the long runs required for climate studies to within a very small error, since these
68 numerical models are designed on the basis of volume integrated tracer conservation.
69 However, this apparent numerical success ignores some difficult theoretical issues with
70 the equation set being numerically solved, related to the properties of seawater, which
71 have only recently been widely recognized as a result of research that resulted in the
72 Thermodynamic Equation of Seawater 2010 (TEOS-10). These issues mean that the
73 intercomparison of different models, and comparison with ocean observations, needs to
74 be undertaken with care.

75 In particular, it is now widely recognized that the traditional measure of heat
76 content in the ocean, the so-called potential temperature, is not a conservative variable
77 (McDougall, 2003). The potential temperature of a mixture of water masses is not the
78 average of the initial potential temperatures, so potential temperature is “produced” or
79 “destroyed” by mixing within the ocean’s interior. This empirical fact is an inherent
80 property of seawater, and so treating potential temperature as a conservative tracer (as
81 well as making certain other assumptions related to the modelling of heat and salt)
82 results in inherent contradictions, which have been built into most ocean models to
83 varying degrees.

84 These contradictions have always existed, but have generally been ignored or
85 overlooked, probably because many other oceanographic factors were thought to be of
86 greater concern. However, as global heat budgets and their imbalances are now a
87 critical factor in understanding changes in climate, it is important to examine the
88 consequences of these assumptions, and perhaps correct them even at the cost of



89 introducing problems elsewhere. This is particularly important when heat budgets are
90 being compared between different models, and with similar calculations made with
91 observed conditions in the real ocean.

92 The purpose of this paper is to describe these theoretical difficulties, to estimate
93 the magnitude of errors that result, and to make recommendations about resolving them
94 both in current and future modelling efforts. For example, the insistence that a model's
95 temperature variable is potential temperature involves errors in the air-sea heat flux in
96 some areas that are as large as the mean rate of global warming. A simple re-
97 interpretation of the model's temperature variable overcomes this inconsistency and
98 allows the coupled ocean-atmosphere model to conserve heat.

99 The reader who wants to skip straight to the recommendations on how the
100 salinity and temperature outputs of CMIP models should be interpreted can go straight
101 to section 6.

102

103 **2. Background**

104 *Thermodynamic measures of heat content*

105 It is well-known that in-situ temperature is not an appropriate measure of the
106 "heat content" of a water parcel because the in situ temperature of a water parcel
107 changes as the ambient pressure changes (i.e. if a water parcel is transported to a
108 different depth in the ocean). This change is of order 0.1C as pressure changes 1000
109 dbar, and is large relative to the precision of 0.01C required to understand deep ocean
110 circulation patterns. The utility of in situ temperature lies in the fact that it is easily
111 measured with a thermometer, and that air-sea boundary heat fluxes are to some degree
112 proportional to in situ temperature differences.

113 Traditionally, potential temperature has been used as an improved measure of
114 ocean heat content. Potential temperature is defined as the temperature that a parcel
115 would have if moved isentropically and without exchange of mass to a fixed reference
116 pressure (usually taken to be surface pressure), and can be calculated from measured
117 ocean in situ temperatures using empirical correlation equations based on laboratory
118 measurements. However, the heat capacity of seawater varies nonlinearly with



119 temperature and salinity (Fig. 1) and this results in non-conservative behavior under
120 mixing (McDougall (2003), section A.17 of IOC et al. (2010)). Thus the potential
121 temperature field in the ocean is subject to internal sources and sinks, and is thus not
122 conservative.

123 With the development of a Gibbs function for seawater, based on empirical fits to
124 measurements of known thermodynamic properties (Feistel (2008), IOC et al, 2010) it
125 became possible to apply a more rigorous theory for quasi-equilibrium thermodynamics
126 to study heat content problems in the ocean. As a practical matter, calculations can now
127 be made that allow for an estimate of the magnitude of non-conservative terms in the
128 current ocean circulation. By integrating over water depth this production rate can be
129 expressed as an equivalent heat flux per unit area.

130 Non-conservation of potential temperature was thus found to be equivalent to a
131 root mean square surface heat flux of about 60 mW m^{-2} (Graham and McDougall, 2013),
132 and an average value of 16 mW m^{-2} (see below) which can be compared to a current
133 estimated global-warming surface heat flux imbalance of about 300 mW m^{-2} (Zanna et
134 al., 2019). These equivalent heat fluxes and subsequent similar values are gathered into
135 Table 1 for reference. In the context of a conceptual ocean model being driven by known
136 heat fluxes, the absence of the non-conservation of potential temperature causes SST
137 errors seasonally in the equatorial region of about 0.5K (i.e. 0.5°C), while the error (in all
138 seasons) at the outflow of the Amazon is 1.8K (see section 9 of McDougall, 2003). With
139 different boundary conditions these temperature errors will show up in different parts
140 of the ocean model.

141 Unfortunately, no single alternative thermodynamic variable has been found that
142 is both independent of pressure, and conservative under mixing. For example, specific
143 entropy is produced in the ocean interior when mixing occurs, with the depth-integrated
144 production being equivalent to an imbalance in the air-sea heat flux of a root mean
145 square value of about 500 mW m^{-2} (Graham and McDougall, 2013), while specific
146 enthalpy is conservative under mixing at constant pressure, but is intrinsically pressure-
147 dependent.



148 However, it was found that a constructed variable, potential enthalpy
149 (McDougall, 2003) has a mean non-conservation error in the global ocean of only about
150 0.3 mW m^{-2} (this is the mean value of an equivalent surface heat flux, equal to the depth
151 integrated interior production of potential enthalpy (Graham and McDougall, 2013)).
152 The potential enthalpy is the enthalpy of a water parcel after being moved isentropically
153 and adiabatically to the reference pressure 0 dbar where the temperature is equal to the
154 potential temperature, θ , of the water parcel:

$$155 \qquad \qquad \qquad \tilde{h}^0(S_A, \theta) = h(S_A, \theta, 0 \text{ dbar}), \qquad (1)$$

156 where the function h is the specific enthalpy of TEOS-10 (defined as a function of
157 Absolute Salinity, in situ temperature and sea pressure) whereas \tilde{h}^0 is the potential
158 enthalpy function and the over-twiddle implies that the temperature input to this
159 function is potential temperature, θ . By way of comparison, the area-averaged
160 geothermal input of heat into the ocean bottom is about 86 mW m^{-2} , and the interior
161 heating of the ocean due to viscous dissipation, is equivalent to a mean surface heat flux
162 of about 3 mW m^{-2} (Graham and McDougall, 2013). Thus potential enthalpy, although
163 not a theoretically ideal conservative parameter, can be treated as one for all practical
164 purposes in ocean circulation problems.

165 Since potential enthalpy is not a widely-understood property, a decision was
166 made in the development of TEOS-10 to define a new variable, called Conservative
167 Temperature, Θ , which would have units of temperature but be proportional to
168 potential enthalpy:

$$169 \qquad \qquad \qquad \Theta = \tilde{\Theta}(S_A, \theta) = \tilde{h}^0(S_A, \theta) / c_p^0, \qquad (2)$$

170 where the proportionality constant $c_p^0 \equiv 3991.867\,957\,119\,63 \text{ J kg}^{-1} \text{ K}^{-1}$, now embedded in
171 the TEOS-10 standard, was chosen so that the average value of Conservative Temperature
172 at the ocean surface matched that of potential temperature. Although in hindsight other
173 choices (e.g., with fewer significant digits) might have been more useful, this value of c_p^0
174 is now built into the TEOS-10 standard and cannot be changed.

175 Note that at specific locations in the ocean, in particular at low salinities and high
176 temperatures, Θ and θ can differ by more than 1°C (Fig. 2); the difference is a strongly



177 nonlinear function of temperature and salinity. Θ is by definition independent of
178 adiabatic and isohaline changes in pressure.

179

180 ***Why is potential temperature not conservative?***

181 This question is answered in sections A.17 and A.18 of the TEOS-10 Manual (IOC
182 et al., 2010) as well as McDougall (2003), Graham and McDougall (2013) and Tailleux
183 (2015). The answer is that potential enthalpy referenced to the sea surface pressure, h^0 ,
184 which is an (almost totally) conservative variable in the real ocean, is not simply a linear
185 function of potential temperature, θ , and Absolute Salinity, S_A (and note that both
186 enthalpy and entropy are unknown and unknowable up to separate linear functions of
187 Absolute Salinity). If potential enthalpy were a linear function of potential temperature
188 and Absolute Salinity then the “heat content” per unit mass of seawater could be
189 accurately taken to be proportional to potential temperature, and the isobaric specific
190 heat capacity at zero sea pressure would be a constant. As an example of the
191 nonlinearity of $\tilde{h}^0(S_A, \theta)$, the isobaric specific heat at the sea surface pressure
192 $c_p(S_A, \theta, 0\text{dbar}) \equiv \tilde{h}_\theta^0$ varies by 6% across the full range of temperatures and salinities
193 found in the World Ocean (Fig. 1). By way of contrast, the potential enthalpy of an ideal
194 gas is proportional to its potential temperature. An early expression for the enthalpy of
195 seawater was published fifty years ago by Connors (1970), and since 2010
196 oceanographers have switched from using potential temperature to Conservative
197 Temperature as part of the switch from EOS-80 to TEOS-10.

198

199 ***How conservative is Conservative Temperature?***

200 This question is addressed in McDougall (2003) as well as in section A.18 of the
201 TEOS-10 Manual (IOC et al., 2010), Graham and McDougall (2013) and Tailleux (2015).
202 Enthalpy is conserved when mixing occurs but enthalpy does not possess the “potential”
203 property, but rather, an adiabatic and isohaline change in pressure causes a change in
204 enthalpy according to $\hat{h}_p = v$, where v is the specific volume. This is illustrated in Fig. 3
205 where it is seen that for an adiabatic and isohaline increase of pressure of 1000dbar, the
206 increase in enthalpy is the same as that caused by an increase in Conservative



207 Temperature of more than 2.4°C. If enthalpy variations at constant pressure were a
208 linear function of Absolute Salinity and Conservative Temperature, the contours in Fig.
209 3 would be parallel equidistant straight lines, and Conservative Temperature would be
210 totally conservative. Since this is not the case, this figure illustrates the (small) non-
211 conservation of Conservative Temperature.

212

213 *Seawater Salinity*

214 To a degree of approximation which is useful for many purposes, the dissolved
215 matter in seawater (“sea salt”) can be treated as a material of uniform composition,
216 whose absolute salinity (i.e. the grams of solute per kilogram of seawater) changes only
217 due to the addition and removal of freshwater through rain, evaporation, and river
218 inflow. This is because the processes that govern the addition and removal of the
219 constituents of sea salt have extremely long time scales, relative to those that affect the
220 pure water component of seawater, so that we can treat the total ocean salt content as
221 approximately constant, while subject to spatially and temporally varying boundary
222 fluxes of fresh water which give rise to salinity gradients.

223 The utility of this definition of uniform composition of sea salt lies in its
224 conceptual simplicity, well suited to theoretical and numerical ocean modelling at time
225 scales of up to 100s of years. However, to the demanding degree required for observing
226 and understanding deep ocean pressure gradients, sea salt is neither uniform in
227 composition, nor is it a conserved variable, nor can its absolute amount be measured
228 precisely in any reasonable manner. The repeatable precision of various technologies
229 used to estimate salinity can be as small as 0.001 g/kg, but the non-ideal nature of
230 seawater means that these estimates can be different by as much as 0.025 g/kg relative to
231 the true Absolute Salinity in the open ocean, and as much 0.1 g/kg in coastal areas
232 (Pawlowicz, 2015).

233 The most important interior source and sink factors governing changes in the
234 composition of sea salt are biogeochemical processes that govern the biological uptake of
235 dissolved nutrients, calcium, and carbon in the upper ocean, and the remineralization of
236 these substances from sinking particles at depth. At present it is thought that changes



237 resulting from hydrothermal vent activity, fractionation from sea ice formation, and
238 through multi-component molecular diffusion processes are of local importance only,
239 but little work has been done to quantify this.

240 In order to address this problem, TEOS-10 defines a Reference Composition of
241 seawater, and a number of slightly different salinity variables that are necessary for
242 different purposes to account for the non-ideal nature of sea salt. The TEOS-10 Absolute
243 Salinity, S_A , is the absolute salinity of Reference Composition Seawater of a measured
244 density (note that capitalization of variable names denotes a precise definition in TEOS-
245 10). It is the only salinity variable that can be properly used in calculations of density
246 using the TEOS-10 Gibbs function. Solution Absolute Salinity, S_A^{soln} , is the (difficult to
247 measure) absolute salinity of a seawater sample whose composition differs from
248 Reference Composition; its use would be limited to budgets of dissolved matter.
249 Preformed Salinity, S_* , is the salinity of a seawater parcel with the effects of
250 biogeochemical processes removed, somewhat analogous to a chlorinity-based salinity
251 estimate. It is thus a conservative tracer of seawater, suitable for modelling purposes,
252 but neglects the spatially-variable small portion of sea salt involved in biogeochemical
253 processes that is required for the most accurate density estimates.

254 Finally, ocean observations require a completely different variable, the Practical
255 Salinity. This variable, which predates TEOS-10, is essentially based on a measure of the
256 electrical conductance of seawater, normalized to conditions of fixed temperature and
257 pressure by empirical correlation equations, and scaled so that ocean salinity
258 measurements that have been made through a variety of technologies over the past 120
259 years are numerically comparable. Practical Salinity measurement technologies involve
260 a certified reference material called IAPSO Standard Seawater, which for our purposes
261 can be considered the best available artifact representing seawater of Reference
262 Composition.

263 Practical Salinity was not designed for numerical modelling purposes and does not
264 accurately represent the mass fraction of dissolved matter. We can link Practical
265 Salinity, S_p , to the Absolute Salinity of Reference Composition seawater (so-called
266 Reference Salinity, S_R) using a fixed scale factor, u_{ps} , so that



267
$$S_R = u_{PS} S_p \quad \text{where} \quad u_{PS} \equiv (35.165\ 04/35) \text{ g kg}^{-1}. \quad (3)$$

268 Conversions to and between the other “salinity” definitions, however, involve
269 knowledge about spatial and temporal variations in seawater composition. Fortunately,
270 the largest component of these changes occurs in a set of constituents involved in
271 biogeochemical processes, whose co-variation is known to be strongly correlated. Thus
272 the Absolute Salinity of real seawater can be determined globally to useful accuracy
273 from the Reference Salinity by the addition of a single parameter, the so-called Absolute
274 Salinity Anomaly, δS_A ,

275
$$S_A = S_R + \delta S_A, \quad (4)$$

276 which has been tabulated in a global atlas for the current ocean (McDougall et al., 2012),
277 and is estimated in coastal areas by considering the effects of river salts (Pawlowicz,
278 2015). It can also be determined from measurements of either density or of carbon and
279 nutrients (IOC et al., 2010). For purposes of numerical ocean modelling, it could in
280 theory be obtained by separately tracking the carbon cycle and nutrients, and applying
281 known correction factors, but we are not aware of any attempts to do so.

282 Finally, chemical modelling (Pawlowicz (2010), Wright et al. (2011), Pawlowicz et
283 al. (2012)) suggests the approximate relation

284
$$S_A - S_* \approx 1.35 \delta S_A \equiv 1.35(S_A - S_R), \quad (5)$$

285 and these relationships are schematically illustrated in Fig. 4. The magnitude of the
286 Absolute Salinity Anomaly is around -0.005 to $+0.025$ g/kg in the open ocean, relative to a
287 mean Absolute Salinity of about 35 g/kg. The correction it implies may be important
288 when initializing models, or comparing them with observations, but its major effect is
289 likely in producing biases in calculated isobaric density gradients.

290

291 *Seawater density*

292 The density of seawater is the most important thermodynamic property affecting
293 oceanic motions, since its spatial changes (along with changes to the sea-surface height)
294 give rise to pressure gradients which are the primary driving force for currents within
295 the ocean interior through the hydrostatic relation. The “traditional” equation of state is
296 known as EOS-80 (UNESCO, 1981), and is standardized as a function of Practical



297 Salinity and in-situ temperature, $\rho = \rho(S_p, t, p)$, which has 41 numerical terms. An
298 additional equation (the adiabatic lapse rate) is required for conversion of temperature
299 to potential temperature. However, for ocean models, the equation of state is usually
300 taken to be the 41-term expression written in terms of potential temperature,
301 $\rho = \tilde{\rho}(S_p, \theta, p)$, of Jackett and McDougall (1995), where the over-twiddle indicates that
302 this rational function fit was made with Practical Salinity S_p and potential temperature
303 θ as the input salinity and temperature variables.

304 The current standard for describing the thermodynamic properties of seawater,
305 known as TEOS-10, provides an equation of state, $v = 1/\rho = v(S_A, t, p)$, in the form of a
306 function which involves 75 coefficients (IOC et al., 2010) and is an analytical pressure
307 derivative of the TEOS-10 Gibbs function. However, for ocean models using TEOS-10
308 the equation of state used is one of those in Roquet et al. (2015); the 55-term equation of
309 state, $\rho = \hat{\rho}(S_A, \Theta, z)$, used by Boussinesq models and the 75-term form in terms of
310 specific volume, $v = \hat{v}(S_A, \Theta, p)$, used by non-Boussinesq ocean models.

311 In this paper we will not concentrate on the distinction between Boussinesq and
312 non-Boussinesq ocean models, and henceforth we will take the third input to the
313 equation of state to be pressure, even though for a Boussinesq model it is in fact a scaled
314 version of depth. By the same token, we will cast the discussion in terms of the in situ
315 density, even though the non-Boussinesq models have as their equation of state a
316 polynomial for the specific volume, $v = 1/\rho$.

317 For seawater of Reference Composition, both the TEOS-10 and EOS-80 fits
318 $\rho = \hat{\rho}(S_A, \Theta, p)$ and $\rho = \tilde{\rho}(S_p, \theta, p)$ are almost equally accurate (see section A.5 of IOC et
319 al. (2010), and in particular, note the comparison between Figures A.5.1 and A.5.2
320 therein). That is, if we set $\delta S_A = 0$ and use Eqn. (3) to relate Practical and Reference
321 Salinities (which in this case are the same as Preformed Salinities), the numerical density
322 values of in situ density calculated using EOS-80 are not significantly different to those
323 using TEOS-10.

324 This being the case, we can see from section A.5 and A.20 of the TEOS-10 Manual
325 (IOC et al. (2010)) that 58% of the data deeper than 1000 dbar in the World Ocean would
326 have the thermal wind misestimated by ~2.7% due to ignoring the difference between



327 Absolute and Reference Salinities. No ocean model has addressed this deficiency to
328 date, but McCarthy et al. (2015) studied the influence of using Absolute Salinity versus
329 Reference Salinity in calculating the overturning circulation in the North Atlantic. They
330 found that the overturning streamfunction changed by 0.7Sv at a depth of 2700m,
331 relative to a mean value at this depth of about 7 Sv, i.e. a 10% effect. Because we argue
332 that the salinity variable in ocean models is best interpreted as being Preformed Salinity,
333 S_* , the neglect of the distinction between Preformed and Absolute Salinities in ocean
334 models means that they mis-estimate the overturning streamfunction by 1.35 (see Figure
335 4) times 0.7Sv, namely ~1Sv, i.e. a 13.5% effect.

336

337 *Air-sea heat fluxes*

338 Sensible, latent and long-wave radiative fluxes are affected by near-surface
339 turbulence and are usually calculated using bulk formulae involving air and sea
340 surface water temperatures (the air and sea in situ temperatures), as well as other
341 parameters (e.g., the latent heat involves the isobaric evaporation enthalpy, commonly
342 called the latent heat of evaporation, which is actually a weak function of temperature
343 and salinity; see Eqn. 6.28 of Feistel et al. (2010) and Eqn. (3.39.7) of IOC et al. (2010)).
344 The total air-sea heat flux, Q , is then translated into a water temperature change by
345 dividing by a heat capacity c_p^0 , which has always been taken to be constant in
346 numerical models (Griffies et al., 2016). Although this is appropriate for CT
347 (assuming that the TEOS-10 value is used for c_p^0), it is not appropriate when potential
348 temperature is being considered. The flux of potential temperature into the surface of
349 the ocean should be Q divided by $c_p(S_*, \theta, 0)$. The use of a constant specific heat
350 capacity, in association with the interpretation of the ocean's temperature variable as
351 being potential temperature, means that the ocean has received a different amount of
352 heat than the atmosphere actually delivers to the ocean, and this issue will be
353 explored in section 3.

354 When precipitation (P) occurs at the sea surface, this addition of freshwater
355 brings with it the associated potential enthalpy $h(S_A=0, t, 0\text{dbar})$ per unit mass of
356 freshwater, where t is the in situ temperature of the rain drops as they arrive at the sea



357 surface. The temperature at which rain enters the ocean is not yet treated consistently in
358 coupled models, and section K1.6 of Griffies et al. (2016) suggests that this effect could
359 be equivalent to an area-averaged extra air-sea heat flux of between -150 mW m^{-2}
360 and -300 mW m^{-2} , representing a heat loss for the ocean.

361

362 *Numerical ocean models*

363 In deciding how to numerically model the ocean, an explicit choice must be made
364 about the equation of state, and one would think that this choice would have
365 implications about the precise meaning of the temperature and salinity variables in the
366 model, which we will call T_{model} and S_{model} respectively. We can divide ocean models
367 into two general classes, EOS-80 models and TEOS-10 models:

368

369 EOS-80 models

370 One class of CMIP models is based around EOS-80, and these models have the
371 following characteristics:

- 372 1. The model's equation of state, $\rho = \tilde{\rho}(S_p, \theta, p)$, expects to have Practical Salinity
373 and potential temperature as the salinity and temperature input parameters.
- 374 2. T_{model} is advected and diffused in the ocean interior in a conservative manner.
- 375 3. S_{model} is advected and diffused in the ocean interior in a conservative manner.
- 376 4. The air-sea heat flux is delivered to/from the ocean using a constant isobaric
377 specific heat, c_p^0 , to convert the air-sea heat flux into a surface flux of T_{model} . [A
378 EOS-80 based model's value of c_p^0 is generally only slightly different than the
379 TEOS-10 value.]
- 380 5. T_{model} is initialized from an atlas of values of potential temperature, and S_{model} is
381 initialized with values of Practical Salinity.

382 Naively, it then seems reasonable to assume that T_{model} is potential temperature, and
383 S_{model} Practical Salinity; but this assumption implies that theoretical errors arising from
384 items 2 and 3 and 4 are ignored (since neither potential temperature nor Practical
385 Salinity are conservative variables). In this paper we show that these interpretations of



386 the model's temperature and salinity variables are not defensible, and we propose
387 alternative interpretations.

388

389 TEOS-10 models

390 Other models have begun to implement TEOS-10 features. These models generally have
391 the following characteristics.

- 392 1. The model's equation of state, $\rho = \hat{\rho}(S_A, \Theta, p)$, expects to have Absolute Salinity
393 and Conservative Temperature as its salinity and temperature input parameters.
- 394 2. T_{model} is advected and diffused in the ocean interior in a conservative manner.
- 395 3. S_{model} is advected and diffused in the ocean interior in a conservative manner.
- 396 4. At each time step of the model, the value of potential temperature at the sea
397 surface (i.e. SST) is calculated from the T_{model} (which is assumed to be
398 Conservative Temperature) and this value of SST is used to interact with the
399 atmosphere via bulk flux formulae.
- 400 5. The air-sea heat flux is delivered to/from the ocean using the TEOS-10 constant
401 isobaric specific heat, c_p^0 , to convert the air-sea heat flux into a surface flux of
402 T_{model} .
- 403 6. T_{model} is initialized from an atlas of values of Conservative Temperature, and
404 S_{model} is initialized with values of one of Absolute Salinity, Reference Salinity or
405 Preformed Salinity.

406 Implicitly, it has then been assumed that T_{model} is a Conservative Temperature, and S_{model}
407 is Absolute Salinity.

408 There is one CMIP6 ocean model that we are aware of, ACCESS-CM2 (Bi et al.
409 2013), whose equation of state is written in terms of Conservative Temperature, but the
410 salinity argument in the equation of state is Practical Salinity. The salinity in this model
411 is initialized with atlas values of Practical Salinity.

412 From the above, it is clear that there are small but significant theoretical
413 incompatibilities between different models, and between models and the actual ocean.
414 These issues become apparent when dealing with the technicalities of intercomparisons,



415 and various choices must be made. We now consider the implications of these different
416 choices.

417

418 3. The Interpretation of salinity in ocean models

419 Note that in both the EOS-80 and TEOS-10 cases, we still have the question of
420 how the salinity variable that is carried in the ocean models of CMIP6 should be
421 interpreted. Consider first the case of the TEOS-10 based models. During the long pre-
422 industrial spin-up period of order a thousand years, the salinity variable in the model is
423 treated as being totally conservative, as is Preformed Salinity, S_* . Whether the model
424 was initialized with values of Absolute Salinity, Reference Salinity or Preformed
425 Salinity, these initial salinity values are nearly identical in the upper ocean, and any
426 differences between the three initial conditions in the deeper ocean would be diffused
427 away within the spin-up period. In the absence of the non-conservative biogeochemical
428 source terms that are needed to force Absolute Salinity away from being conservative
429 and towards the observed values of Absolute Salinity (or the smaller source terms that
430 are needed to maintain Reference Salinity) the model's salinity variable will drift away
431 from the initial condition and will behave as a conservative salinity variable. Hence we
432 conclude that the salinity variable that a TEOS-10 based model contains after the long
433 spin-up phase is Preformed Salinity S_* , irrespective of whether the model was
434 initialized with values of Absolute Salinity, Reference Salinity or Preformed Salinity.

435 Likewise, the prognostic salinity variable after a long spin-up period of an EOS-
436 80 based model is most accurately interpreted as being Preformed Salinity divided by
437 $u_{\text{PS}} \equiv (35.165\ 04/35) \text{ g kg}^{-1}$, S_*/u_{PS} .

438 We clearly need more estimates of the magnitude of the dynamic effects of the
439 variable seawater composition, but for now we might take a change in 1 Sv in the
440 meridional transport of deep water masses in each ocean basin (based on the work of
441 McCarthy et al., 2015) as an indication of the magnitude of the effect of neglecting the
442 effects of biogeochemistry on salinity. At this stage of model development, since all
443 models are equally deficient in their thermophysical treatment of salinity, at least this
444 aspect does not present a problem as far as making comparisons between CMIP models.



445

446 **4. Model Heat Flux Calculations**

447 It is clear from the details described above that both types of numerical ocean models
448 suffer from some internal contradictions with thermodynamical best practice. For
449 example, for the EOS-80 based models, if T_{model} is assumed to be potential temperature,
450 the use of EOS-80 is correct for density calculations but the use of conservative equations
451 for T_{model} ignores the non-conservative production of potential temperature. The use of a
452 constant heat capacity is also in error if T_{model} is interpreted as potential temperature.
453 Conservative equations are, however, appropriate for Conservative Temperature. In
454 addition, if S_{model} is assumed to be either Practical Salinity or Absolute Salinity, then the
455 use of conservative equations ignores the changes in salinity that arise from
456 biogeochemical processes.

457 One use for these models is to calculate heat budgets and heat fluxes – both at the
458 surface and between latitudinal bands, and inherent to CMIP is the idea that these
459 different models should be intercompared. The question of how this intercomparison
460 should be done, however, was not clearly addressed in Griffies et al. (2016). Here we
461 begin the discussion by considering two different options for interpreting T_{model} in EOS-
462 80 ocean models.

463

464 ***4.1 Option 1: interpreting the EOS-80's model's temperature as being potential***

465 ***temperature***

466 Under this option the model's temperature variable T_{model} is treated as being potential
467 temperature θ ; this is the prevailing interpretation to date. With this interpretation of
468 T_{model} one wonders whether Conservative Temperature Θ should be calculated from the
469 model's (assumed) potential temperature before calculating (i) the global Ocean Heat
470 Content as the volume integral of $\rho c_p^0 \Theta$, and (ii) the advective meridional heat transport
471 as the area integral of $\rho c_p^0 \Theta v$ at constant latitude, where v is the northward velocity.
472 This question was not clearly addressed in Griffies et al. (2016), and here we emphasize
473 one of the main conclusions of the present paper, namely that ocean heat content and
474 meridional heat transports should be calculated using the model's prognostic



475 temperature variable. Any subsequent conversion from one temperature variable to
476 another (such as potential to Conservative) in order to calculate heat content and heat
477 transport is incorrect and confusing, and should not be attempted.

478

479 *4.1.1 Issues with the potential temperature interpretation*

480 There are several thermodynamic inconsistencies that arise from option 1. First,
481 the ocean model has assumed in its spin-up phase (for perhaps a millennium) that
482 potential temperature is conservative, so during the whole spin-up phase and beyond,
483 the contribution of the known non-conservative interior source terms of potential
484 temperature have been absent, and hence the model's temperature variable has not
485 responded to these absent source terms and so this temperature field cannot be potential
486 temperature. Also, since the temperature field of the model is not potential temperature
487 (because of these absent source terms) the velocity field of the model will also not be
488 forced correctly due to errors in the density field which in turn affect the pressure force.

489 The second inconsistent aspect of option 1 is that the air-sea flux of heat is
490 ingested into the ocean model, both during the spin-up stage and during the transient
491 response phase, as though the model's temperature variable is proportional to potential
492 enthalpy. For example, consider some time during the year at a particular location
493 where the sea surface is fresh (a river outflow, or melted ice). During this time, any heat
494 that the atmosphere loses or gains should have affected the potential temperature of the
495 upper layers of the ocean using a specific heat that is 6% larger than c_p^0 (see Figure 1).
496 So if the ocean model's temperature variable is interpreted as being potential
497 temperature, a 6% error is made in the heat flux that is exchanged with the atmosphere
498 during these periods/locations. That is, the changes in the ocean model's (assumed)
499 potential temperature caused by the air-sea heat flux will be exaggerated where and
500 when the sea surface salinity is relatively fresh. This 6% flux error is not corrected by
501 subsequently calculating Conservative Temperature from potential temperature; for
502 example, these temperatures are the same at low temperature and salinity (see Figure 2),
503 and yet at low values of salinity, the specific heat is 6% larger than c_p^0 .



504 This second inconsistent aspect of option 1 can be restated as follows. The
505 adoption of potential temperature as the model's temperature variable means that there
506 is a discontinuity in the heat flux of the coupled air-sea system right at the sea surface;
507 for every Joule of heat (i.e. potential enthalpy) that the atmosphere gives to the ocean,
508 under this Option 1 interpretation, up to 6% too much heat arrives in the ocean over
509 relatively fresh waters. In this way, the adoption of potential temperature as the model
510 temperature variable ensures that the coupled ocean atmosphere system will not
511 conserve heat. Rather, there appear to be non-conservative sources and sinks of heat
512 right at the sea surface where heat is unphysically manufactured or destroyed.

513 The third inconsistent aspect is a direct consequence of the second; namely that if
514 one is tempted to post-calculate Conservative Temperature Θ from the model's
515 (assumed) values of potential temperature, the calculated ocean heat content as the
516 volume integral of $\rho c_p^0 \Theta$ would no longer be accurately related to the heat that the
517 atmosphere exchanged with the ocean. Neither would the area integral between latitude
518 bands of the air-sea heat flux be exactly equal to the difference between the calculated
519 meridional heat transports that cross those latitudes. Rather, during the running of the
520 model the heat that was lost from the atmosphere actually shows up in the ocean as the
521 volume integral of the model's prognostic temperature variable. We agree with
522 Appendix D3.3 of Griffies et al. (2016) and strongly recommend that Conservative
523 Temperature is not calculated a posteriori in order to evaluate heat content and heat
524 fluxes in these EOS-80 based models.

525

526 4.1.2 Quantifying the air-sea flux imbalance

527 Here we quantify the air-sea flux errors involved with assuming that T_{model} of
528 EOS-80 models is potential temperature. These EOS-80 based models calculate the air-
529 sea flux of their model's temperature as the air-sea heat flux, Q , divided by c_p^0 .
530 However, since the isobaric specific heat capacity of real seawater is $c_p(S_*, \theta, 0)$, the flux
531 of potential temperature into the surface of the ocean should be Q divided by $c_p(S_*, \theta, 0)$.
532 So, if the model's temperature variable is interpreted as being potential temperature, the
533 EOS-80 model has a flux of potential temperature entering the ocean that is too large by



534 the difference between these transports, namely by Q/c_p^0 minus $Q/c_p(S_*,\theta,0)$. This
535 means that the ocean has received a different amount of heat than the atmosphere
536 actually delivers to the ocean, with the difference, ΔQ , being $c_p(S_*,\theta,0)$ times the
537 difference in the surface fluxes of potential temperature, namely (for the last part of this
538 equation, see Eqn. (A.12.3a) of IOC et al., 2010)

$$539 \quad \Delta Q = Q \left(\frac{c_p(S_*,\theta,0)}{c_p^0} - 1 \right) = Q(\tilde{\Theta}_\theta - 1). \quad (6)$$

540 We plot this quantity from the pre-industrial control run of ACCESS-CM2 in
541 Figure 5c and show it as a cell area-weighted histogram in Figure 5e (note that while
542 these plots apply to EOS-80 based ocean models, to generate these plots we have
543 actually used data from ACCESS-CM2 which is a mostly TEOS-10 compliant model).
544 The calculation takes into account the penetration of shortwave radiation into the ocean
545 but is performed using monthly-averages of the thermodynamics quantities. The
546 temperatures and salinities at which the radiative flux divergences occur are taken into
547 account in this calculation, but the result is little changed if the sea surface temperatures
548 and salinities are used with the radiative flux divergence assumed to take place at the
549 sea surface. Results from similar calculations performed using monthly and daily-
550 averaged quantities in ACCESS-OM2 (Kiss et al. 2020) ocean-only model simulations
551 were similar, suggesting that correlations between sub-monthly variations are not
552 significant (at least in these relatively coarse-resolution, diffuse models).

553 ΔQ has an area-weighted mean value of 16 mW m^{-2} and we know that this
554 represents the net surface flux of potential temperature required to balance the volume
555 integrated non-conservation of potential temperature in the ocean's interior (Tailleux
556 (2015)). To put this value in context, 16 mW m^{-2} corresponds to 5% of the observed trend
557 of 300 mW m^{-2} in the global ocean heat content from 1955-2017 (Zanna et al. 2019). In
558 addition to this mean value of ΔQ , we see from Figure 5c that there are small regions
559 such as the equatorial Pacific and the western north Pacific where ΔQ is as large as the
560 area-averaged heat flux, 300 mW m^{-2} , that the ocean has received since 1955. These local
561 anomalies of air-sea flux, if they actually existed, would drive local variations in
562 temperature. However, these ΔQ values do not represent real heat fluxes. Rather they



563 represent the error in the air-sea heat flux that we make if we insist that the temperature
564 variable in an EOS-80 based ocean model is potential temperature, with the ocean
565 receiving a surface heat flux that is larger by ΔQ than the atmosphere delivers to the
566 ocean. Figure 6 shows the zonal integration of ΔQ , in units of W per degree of latitude.

567 Figure 5e shows that, with T_{model} being interpreted as potential temperature, 5%
568 of the surface area of the ocean needs a surface heat flux that is more than 135 mW m^{-2}
569 different to what the atmosphere gives to/from the ocean. This regional variation of ΔQ
570 of approximately $\pm 100 \text{ mW m}^{-2}$ is consistent with the regional variations in air-sea flux of
571 potential temperature found by Graham and McDougall (2013) that is needed to balance
572 the depth-integrated non-conservation of potential temperature as a function of latitude
573 and longitude. Figures 5d,f show that much of this spread is due to the variation of the
574 isobaric specific heat capacity on salinity, with the remainder due to the variation of this
575 heat capacity with temperature. We note that if this analysis were performed with a
576 model that resolved individual rain showers, then these episodes of very fresh water at
577 the sea surface would be expected to increase the calculated values of ΔQ . Interestingly,
578 by way of contrast, it is the variation of the isobaric heat capacity with temperature that
579 dominates (by a factor of four) the contribution of this heat capacity variation to the area
580 mean of ΔQ (with the contribution of salinity, ΔQ_s , in Figure. 5d, leading to an area
581 mean of 4 mW m^{-2}), as originally found by Tailleux (2015).

582 While a heat flux error of $\pm 100 \text{ mW m}^{-2}$ is not large, it also not trivially small, and
583 it seems advisable to respect these fundamental thermodynamic aspects of the coupled
584 earth system. We will see that this $\pm 100 \text{ mW m}^{-2}$ issue is simply avoided by realizing
585 that the temperature variable in these EOS-80 models is not potential temperature.

586 In Appendix A we enquire whether the way that EOS-80 models treat their fluid
587 might be made to be thermodynamically correct for a fluid other than seawater. We find
588 that it is possible to construct such a thermodynamic definition of a fluid with the aim
589 that its treatment in EOS-80 models is consistent with the laws of thermodynamics. This
590 fluid has the same specific volume as seawater for given values of salinity, potential
591 temperature and pressure, but it has different expressions for both enthalpy and
592 entropy. This fluid also has a different adiabatic lapse rate and therefore a different



593 relationship between in situ and potential temperatures. However this exercise in
594 thermodynamic abstraction does not alter the fact that, as a model of the real ocean, and
595 with the temperature variable being interpreted as being potential temperature, the
596 EOS-80 models have ΔQ more heat arriving in the ocean than leaves the atmosphere.

597 Since CMIP6 is centrally concerned with how the planet warms, it seems
598 advisable to adopt a framework where heat fluxes and their consequences are respected.
599 That is, we regard it as imperative to avoid non-conservative sources of heat at the sea
600 surface. It is the insistence that the temperature variable in EOS-80 based models is
601 potential temperature that implies that the ocean receives a heat flux from the
602 atmosphere that is larger by ΔQ than what the atmosphere actually exchanges with the
603 ocean. Since there are some areas of the ocean surface where ΔQ is as large as the mean
604 rate of global warming, Option 1 is not supportable. This is what motivates Option 2
605 where we change the interpretation of the model's temperature variable from being
606 potential temperature to Conservative Temperature.

607

608 **4.2 Option 2: interpreting the EOS-80's model's temperature as being Conservative**

609 **Temperature**

610 Under this option the ocean model's temperature variable is taken to be Conservative
611 Temperature Θ . The air-sea flux of potential enthalpy is then correctly ingested into the
612 ocean model using the fixed specific heat c_p^0 , and the mixing processes in the model
613 correctly conserve Conservative Temperature. Hence the second, fourth and fifth items
614 listed in section 2 are handled correctly, except for the following caveat. In the coupled
615 model, the bulk formulae that set the air-sea heat flux at each time step use the
616 uppermost model temperature as the sea surface temperature as input. So with the
617 Option 2 interpretation of the model's temperature variable as being Conservative
618 Temperature, these bulk formulae are not being fed the SST (which at the sea surface is
619 equal to the potential temperature θ). The difference between these temperatures is
620 $\Theta - \theta$, which is the negative of what we plot in Figure 2. This is a caveat with this
621 Option 2 interpretation, namely that the bulk formula that the model uses to determine
622 the air-sea flux at each time step is actually a little bit different to what was intended



623 when the parameters of the bulk formulae were chosen. This is a caveat regarding what
624 was intended by the coupled modeler, rather than what the coupled model actually
625 experienced. That is, with this Option 2 interpretation, the air-sea heat flux, while being
626 a little bit different than what might have been intended, does arrive in the ocean
627 properly; there is no non-conservative production or destruction of heat at the air-sea
628 boundary as there is in Option 1.

629 Regarding the remaining two items involving temperature listed in section 2, we
630 can dismiss the fifth item, since any small difference in the initial values, set at the
631 beginning of the lengthy spin-up period, between potential temperature and
632 Conservative Temperature will be irrelevant after the long spin-up integration.

633 This leaves the first point, namely that the model used the equation of state that
634 expects potential temperature as its temperature input, $\tilde{\rho}(S_*/u_{ps}, \theta, p)$, but under this
635 Option 2 we are interpreting the model's temperature variable as being Conservative
636 Temperature. In the remainder of this section we address the magnitude of this effect,
637 namely, the use of $\tilde{\rho}(S_*/u_{ps}, \Theta, p)$ versus the correct density $\tilde{\rho}(S_*/u_{ps}, \theta, p)$ which is
638 almost the same as $\hat{\rho}(S_*, \Theta, p)$. Note, as discussed in section 3 above, the salinity
639 argument of the TEOS-10 equation of state is taken to be S_* while that of the EOS-80
640 equation of state is taken to be S_*/u_{ps} . These salinity variables are simply proportional
641 to each other, and they have the same influence in both equations of state.

642 Under this Option 2 we are interpreting the model's temperature variable as
643 being Conservative Temperature, and so the density value that the model calculates
644 from its equation of state is deemed to be $\tilde{\rho}(S_*/u_{ps}, \Theta, p)$ whereas the density should be
645 evaluated as $\hat{\rho}(S_*, \Theta, p)$ where we remind ourselves that the hat over the in situ density
646 function indicates that this is the TEOS-10 equation of state, written with Conservative
647 Temperature as its temperature input. To be clear, under EOS-80 and under TEOS-10
648 the in situ density of seawater of Reference Composition has been expressed by two
649 different expressions,

$$650 \quad \rho = \tilde{\rho}(S_*/u_{ps}, \theta, p) = \hat{\rho}(S_*, \Theta, p), \quad (7)$$

651 both of which are very good fits to the in situ density (hence the equals signs); the
652 increased accuracy of the TEOS-10 equation for density was mostly due to the



653 refinement of the salinity variable, and the increase in the accuracy of TEOS-10 versus
 654 EOS-80 for Standard Seawater (Millero et al., 2008) was minor by comparison.

655 So we need to ask what error will arise from calculating in situ density in the
 656 model as $\tilde{\rho}(S_*/u_{ps}, \Theta, p)$ instead of as the correct TEOS-10 version of in situ density,
 657 $\hat{\rho}(S_*, \Theta, p)$? The effect of this small difference on calculations of the buoyancy frequency
 658 and even the neutral tangent plane is likely small, so we concentrate on the effect of this
 659 difference on the isobaric gradient of in-situ density (the thermal wind).

660 Given that under this Option 2 the model's temperature variable is being
 661 interpreted as Conservative Temperature, Θ , the model-calculated isobaric gradient of
 662 in-situ density is

$$663 \quad \tilde{\rho}_{S_*} \nabla_p S_* + \tilde{\rho}_{\Theta} \nabla_p \Theta, \quad (8)$$

664 whereas the correct isobaric gradient of in-situ density is actually

$$665 \quad \hat{\rho}_{S_*} \nabla_p S_* + \hat{\rho}_{\Theta} \nabla_p \Theta. \quad (9)$$

666 Notice that here and henceforth we drop the scaling factor u_{ps} from the gradient
 667 expressions such as Eqn. (5). In any case, this scaling factor cancels from the expression,
 668 but we simply drop it for ease of looking at the equations; we can imagine that the EOS-
 669 80 equation of state is written in terms of S_* (which would simply require that a first
 670 line is added to the code which divides the salinity variable by u_{ps}).

671 The model's error in evaluating the isobaric gradient of in situ density is then the
 672 difference between the two equations above, namely

$$673 \quad \text{error in } \nabla_p \rho = \left(\tilde{\rho}_{S_*} - \hat{\rho}_{S_*} \right) \nabla_p S_* + \left(\tilde{\rho}_{\Theta} - \hat{\rho}_{\Theta} \right) \nabla_p \Theta. \quad (10)$$

674 The relative error here in the temperature derivative of the equations of state can be
 675 written approximately as

$$676 \quad \left(\tilde{\rho}_{\Theta} - \hat{\rho}_{\Theta} \right) / \hat{\rho}_{\Theta} = \tilde{\alpha}^{\theta} / \hat{\alpha}^{\theta} - 1, \quad (11)$$

677 which is the difference from unity of the ratio of the thermal expansion coefficient with
 678 respect to potential temperature to that with respect to Conservative Temperature. This
 679 ratio, $\tilde{\alpha}^{\theta} / \hat{\alpha}^{\theta}$, can be shown to be equal to $c_p(S_*, \theta, 0) / c_p^0$ and we know (from Figure 1)
 680 that this varies by 6% in the ocean. This ratio is plotted in Figure 7(a). In regions of the
 681 ocean that are very fresh, a relative error in the contribution of the isobaric temperature



682 gradient to the thermal wind will be as large as 6% while in most of the ocean this
683 relative error will be less than 0.5%.

684 Now we turn our attention to the relative error in the salinity derivative of the
685 equation of state, which, from Eqn. (10) can be written approximately as

$$686 \quad \left(\tilde{\rho}_{s_*} - \hat{\rho}_{s_*} \right) / \hat{\rho}_{s_*} = \tilde{\beta}^\theta / \hat{\beta}^\theta - 1, \quad (12)$$

687 and the ratio, $\tilde{\beta}^\theta / \hat{\beta}^\theta$, has been plotted (at $p = 0$ dbar) in Figure 7(b). This figure shows
688 that the relative error in the salinity derivative, $\left(\tilde{\rho}_{s_*} - \hat{\rho}_{s_*} \right) / \hat{\rho}_{s_*}$, is an increasing
689 (approximately quadratic) function of temperature, being approximately zero at 0°C, 1%
690 error at 20°C and 2% error at 30°C. An alternative derivation of these implications of
691 Eqn. (10) is given in Appendix B.

692 We conclude that under Option 2, where the temperature variable of an EOS-80
693 based model (whose polynomial equation of state expects to have potential temperature
694 as its input temperature) is interpreted as being Conservative Temperature, there are
695 persistent errors in the contribution of the isobaric salinity gradient to the isobaric
696 density gradient that are approximately proportional to temperature squared, with the
697 error being approximately 1% at a temperature of 20°C (mostly due to the salinity
698 derivative of in situ density at constant potential temperature being 1% different to the
699 corresponding salinity derivative at constant Conservative Temperature). Larger
700 fractional errors in the contribution of the isobaric temperature gradient to the thermal
701 wind equation do occur (of up to 6%) but these are restricted to the rather small volume
702 of the ocean that is quite fresh.

703 In Figure 8 we have evaluated how much the meridional isobaric density
704 gradient changes in the upper 1000 dbar of the world ocean when the temperature
705 argument in the expression for density is switched from θ to Θ . As explained above,
706 this is almost equivalent to the density difference between calling the EOS-80 and the
707 TEOS-10 equations of state, using the same numeric inputs for each. We find that 19% of
708 this data has the isobaric density gradient changed by more than 1% when switching
709 from θ to Θ . The median value of the percentage error is 0.22%; that is, 50% of the data
710 shallower than 1000 dbar has the isobaric density gradient changed by more than 0.22%



711 when switching from using EOS-80 to TEOS-10, with the same numerical temperature
712 input, which we are interpreting as being Θ .

713

714 **4.3 Evaluating the options for EOS-80 models**

715 Under option 1 where T_{model} is interpreted as potential temperature, there is a
716 non-conservation of heat at the sea surface, with the ocean seeing one heat flux, and the
717 atmosphere immediately above it seeing another, with the differences being typically
718 $\pm 100 \text{ mW m}^{-2}$, with a net imbalance of 16 mW m^{-2} .

719 Under option 2 where T_{model} is interpreted as Conservative Temperature, this flux
720 imbalance does not arise, but two other inaccuracies arise. First, under option 2 the bulk
721 formulae that determine part of the air-sea flux is based on the surface values of Θ
722 rather than of θ (for which the bulk formulae are designed). Second, the isobaric
723 density gradient in the upper ocean is typically different by $\sim 1\%$ to the isobaric density
724 gradient that would be found if the TEOS-10 equation of state had been adopted in these
725 models. These two aspects of option 2 are considered less serious than not conserving
726 heat at the sea surface by $\pm 100 \text{ mW m}^{-2}$. Neither of the two inaccuracies that arise under
727 option 2 are fundamental thermodynamic errors. Rather they are equivalent to the
728 ocean modeler choosing (i) a slightly different bulk formulae, and (ii) a slightly different
729 equation of state. The constants in the bulk formulae are very poorly known so that the
730 switching from θ to Θ in their use will be well within their uncertainty (Cronin et al.,
731 2019) while the $\sim 1\%$ change to the isobaric density gradient due to using the different
732 equations of state is at the level of our knowledge of the equation of state of sea water.

733 We conclude that option 2 where the T_{model} in EOS-80 models is interpreted as
734 Conservative Temperature is much preferred as it treats the air-sea heat flux in a manner
735 consistent with the First Law of Thermodynamics, and the treatment of T_{model} as being a
736 conservative variable is consistent with it being Conservative Temperature.

737

738



739 5. Comparison with ocean observations

740 Now that we have argued that T_{model} should be interpreted as being Conservative
741 Temperature, how then should the model-based estimates of ocean heat content and
742 ocean heat flux be compared with ocean observations and ocean atlas data? The answer
743 is by evaluating the ocean heat content correctly in the observed data sets using TEOS-
744 10, whereby the observed data is used to calculate Conservative Temperature, and this is
745 used together with c_p^0 to evaluate ocean heat content and meridional heat fluxes.

746 We have made the case that the salinity variable in CMIP ocean models that have
747 been spun up for several centuries is Preformed Salinity S_* for the TEOS-10 compliant
748 models, and is S_*/u_{ps} for the EOS-80 compliant models. It is the value of either S_* or
749 S_*/u_{ps} calculated from ocean observations to which the model salinities should be
750 compared. Preformed Salinity S_* is different to Reference Salinity S_{R} by only the ratio
751 $0.26 = 0.35/1.35$ compared with the difference between Absolute Salinity and Preformed
752 Salinity (see Figure 4), and these differences are generally only significantly different to
753 zero at depths exceeding 500 m. Note that Preformed Salinity can be evaluated from
754 observations of Practical Salinity using the Gibbs SeaWater (GSW) software
755 `gsw_Sstar_from_SP`.

756

757 6. Discussion and Recommendations

758 We have made the case that it is advisable to avoid non-conservative sources of
759 heat at the sea surface. It is the prior interpretation of the temperature variable in EOS-
760 80 based models as being potential temperature that implies that the ocean receives a
761 heat flux that is larger by ΔQ than the heat that is lost from the atmosphere. Since there
762 are some areas of the ocean surface where ΔQ is as large as the mean rate of global
763 warming, the issue is not unimportant. This realization has motivated the new
764 interpretation of the prognostic temperature of EOS-80 ocean models as being
765 Conservative Temperature (our option 2).

766 A consequence of this new interpretation of the prognostic temperature variable
767 of all CMIP ocean models as being Conservative Temperature means that the EOS-80
768 based models suffer a relative error of ~1% in their isobaric gradient of in situ density in



769 the warm upper ocean. How worried should we be about this? One perspective on this
770 question is to simply note (from above) that there are larger relative errors (~2.7%) in the
771 thermal wind equation in the deep ocean due to the neglect of variations in the relative
772 composition of seasalt. Another perspective is to ask how well does science even know
773 the thermal expansion coefficient, for example. From appendices K and O of IOC et al.
774 (2010) (and section 7 of McDougall and Barker (2011)) we see that the rms value of the
775 differences between the individual laboratory-based data points of the thermal
776 expansion coefficient and the thermal expansion coefficient obtained from the fitted
777 TEOS-10 Gibbs function is $0.73 \times 10^{-6} \text{ K}^{-1}$ which is approximately 0.5% of a typical value
778 of the thermal expansion coefficient in the ocean. Without a proper estimation of the
779 number of degrees of freedom represented by the fitted data points, we might estimate
780 the relative error of the thermal expansion coefficient obtained from the fitted TEOS-10
781 Gibbs function as being half of this, namely 0.25%. So a typical relative error in the
782 isobaric density gradient of ~1% in the upper ocean due to using Θ rather than θ as the
783 temperature input seems undesirable but not serious.

784 We must also acknowledge that all models have ignored the difference between
785 Preformed Salinity, Reference Salinity and Absolute Salinity (which is the salinity
786 variable from which density is accurately calculated). As discussed in IOC et al. (2010),
787 Wright et al. (2011) and McDougall and Barker (2011), glossing over these issues of the
788 spatially variable composition of sea salt, which is the same as glossing over the effects
789 of biogeochemistry on salinity and density, means that all of our ocean and climate
790 models have errors in their thermal wind (vertical shear of horizontal velocity) that
791 globally exceed 2.7% for half the ocean volume deeper than 1000 m. In the deep North
792 Pacific ocean, the misestimation of thermal wind is many times this 2.7% figure. The
793 recommended way of incorporating the spatially varying composition of seawater into
794 ocean models appears as section A.20 in the TEOS-10 Manual (IOC et al. (2010)), and as
795 section 9 in the McDougall and Barker (2012), with ocean models needing to carry a
796 second salinity type variable. While it is true that this procedure has the effect of
797 relaxing the model towards the non-standard seawater composition of today's ocean, it
798 is clearly advantageous to make a start with this issue by incorporating the non-



799 conservative source terms that apply to the present ocean rather than to continue to
800 ignore the issue altogether. As explained in these references, once the modelling of
801 ocean biogeochemistry matures, the difference between the various types of salinity can
802 be calculated in real time in an ocean model without the need of referring to historical
803 data.

804 Nevertheless, we acknowledge that no ocean model to date has attempted to
805 include the influence of biogeochemistry on salinity and density, and so this is why we
806 recommend that the salinity from both observations and model output be treated as
807 Preformed Salinity S_* .

808

809 **6.1 Contrasts to the recommendations of Griffies et al. (2016)**

810 How does this paper differ from the recommendations in Griffies et al. (2016)?
811 That paper recommended that the ocean heat content and meridional transport of heat
812 should be calculated using the model's temperature variable and the model's value of
813 c_p^0 , and we strenuously agree. However, in the present paper we argue that the
814 temperature variable carried by an EOS-80 based ocean model should be interpreted as
815 being Conservative Temperature, and not be interpreted as being potential temperature.
816 This idea was raised as a possibility in Griffies et al. (2016), but the issue was left unclear
817 in that paper. For example, section D2 of Griffies et al. (2016) recommends that TEOS-10
818 based models archive potential temperature (as well as their model variable,
819 Conservative Temperature) "in order to allow meaningful comparisons" with the output
820 of the EOS-80 based models. We now disagree with this suggestion. The thesis of the
821 present paper is that the temperature variables of both EOS-80 and TEOS-10 based
822 models are already directly comparable, and they should both be interpreted as being
823 Conservative Temperature, and they should both be compared with Conservative
824 Temperature from observations. The fact that the model's temperature variable is
825 labeled "theta0" in EOS-80 models and "THETA" in TEOS-10 based models, we now see
826 as very likely to cause confusion, since we are recommending that the temperature
827 outputs of both types of ocean models should be interpreted as Conservative
828 Temperature.



829 The present paper also diverges from Griffies et al. (2016) in the way that the
830 salinity variables in CMIP ocean models should be interpreted and thus compared to
831 observations. Griffies et al. (2016) interpret the salinity variable in TEOS-10 based ocean
832 models as being Reference Salinity S_r whereas we show that these models actually
833 carry Preformed Salinity S_* but have errors in their calculation of densities. Similarly,
834 Griffies et al. (2016) interpret the salinity variable in EOS-80 based ocean models as being
835 Practical Salinity S_p whereas we show that these models actually carry S_*/u_{ps} , that is,
836 Preformed Salinity divided by the constant, u_{ps} . This distinction between the present
837 paper and Griffies et al. (2016) is negligible in the upper ocean where Preformed Salinity
838 is almost identical to Reference Salinity (because the composition of seawater in the
839 upper ocean is close to Reference Composition), but in the deeper parts of the ocean, the
840 distinction is not negligible; for example, based on the work of McCarthy et al. (2015) we
841 have shown that the use of Absolute Salinity versus Preformed Salinity leads to ~ 1 Sv
842 difference in the meridional overturning streamfunction in the North Atlantic at a depth
843 of 2700 m. However, in this deeper part of the ocean, even though the difference
844 between Absolute Salinity and Preformed Salinity is not negligible, the difference
845 between Preformed Salinity and Reference Salinity (which the TEOS-10 based ocean
846 models have to date assumed their salinity variable to be) is smaller in the ratio $0.35/1.35$
847 $= 0.26$ (see Figure 4). That is, if the salinity output of a TEOS-10 based ocean model was
848 taken to be Reference Salinity, the error would be only a quarter of the difference
849 between Absolute Salinity and Preformed Salinity, a difference which limits the
850 accuracy of the isobaric density gradients in the deeper parts of ocean models (see
851 Figure 4). A similar remark applies to EOS-80 based ocean models if their salinity
852 output is regarded as being Practical Salinity instead of being (as we decree) S_*/u_{ps} .

853

854 **6.2 Summary table of ocean heat content imbalances**

855 In Table 1 we summarize the effects of uncertainties in physical or numerical processes
856 in estimating ocean heat content or its changes. The first two rows are the rate of
857 warming (expressed in mWm^{-2} averaged over the sea surface) due to anthropogenic
858 global warming, and due to geothermal heating. The third row is an estimate of the



859 surface heat flux equivalent of the depth-integrated rate of dissipation of turbulent
860 kinetic energy, and the fourth is an estimate of the neglected net flux of potential
861 enthalpy at the sea surface due to the evaporation and precipitation of water occurring
862 at different temperatures.

863 The next (fifth) row is the consequence of considering the scenario where all of
864 radiant heat is absorbed into the ocean at a pressure of 25 dbar rather than at the sea
865 surface. The derivative of specific enthalpy with respect to Conservative Temperature at
866 25 dbar, \hat{h}_θ , is c_p^0 times the ratio of the absolute in situ temperature at 25 dbar, $(T_0 + t)$,
867 to the absolute potential temperature, $(T_0 + \theta)$ at this pressure (see Eqn. (A.11.15) of IOC
868 et al. (2010)). The ratio of \hat{h}_θ to c_p^0 at 25 dbar is typically different to unity by 6×10^{-6} ,
869 and taking a typical rate of radiative heating of 100 Wm^{-2} over the ocean's surface leads
870 to 0.6 mWm^{-2} as the area-averaged rate of mis-estimation of the surface flux of
871 Conservative Temperature for this assumed pressure of penetrative radiation. Since this
872 is so small, the use of c_p^0 (rather than \hat{h}_θ) to convert the divergence of the radiative heat
873 flux into a flux of Conservative Temperature is well supported, providing the correct
874 diagnostics are used for the calculation (such diagnostic issues may be responsible for
875 the heat budget closure issues identified by Irving et al. 2020).

876 The next six rows of Table 1 list the mean and twice the standard deviation of the
877 volume integrated non-conservation production of Conservative Temperature, potential
878 temperature, and specific entropy, all expressed in mWm^{-2} at the sea surface. The
879 following two rows are the results we have found in this paper for the air-sea heat flux
880 error that is made if the EOS-80's temperature is taken to be potential temperature.

881 The final three rows show that ocean models, being cast in divergence form with
882 heat fluxes being passed between one grid box and the next, do not have appreciable
883 numerical errors in deducing air-sea fluxes from changes in the volume integrated heat
884 content.

885 The estimate from Graham and McDougall (2013) of -10 mWm^{-2} is for the net
886 interior production of θ , so this is a net destruction. A steady state requires this amount
887 of extra flux of θ at the sea surface (so it can be consumed in the interior). Our estimate



888 of this extra flux of θ at the sea surface is 16 mWm^{-2} , which is only a little larger than the
889 estimate of Graham and McDougall (2013).

890

891 **6.3 Summary of recommendations**

892 In summary, this paper has argued for the following simple guidelines for
893 analyzing the CMIP model runs. We should

- 894 1. interpret the prognostic temperature variable of all CMIP models (whether they
895 are based on the EOS-80 or the TEOS-10 equation of state) as being Conservative
896 Temperature,
- 897 2. compare the model's prognostic temperature with the Conservative
898 Temperature, Θ , of observational data,
- 899 3. calculate the ocean heat content as the volume integral of the product of
900 (i) in situ density (ii) the model's prognostic temperature, Θ , and (iii) the model's
901 value of c_p^0 ,
- 902 4. interpret the salinity variable of the model output as being Prefomed Salinity S_*
903 for TEOS-10 based ocean models, and S_*/u_{ps} for EOS-80 based ocean models, (so
904 it is advisable to post-multiply the salinity output of EOS-80 models by u_{ps} in
905 order to have the salinity outputs of all types of CMIP models as Prefomed
906 Salinity S_*) and,
- 907 5. compare the model's salinity variable with Prefomed Salinity, S_* , calculated
908 from ocean observations.
- 909 6. Sea surface temperature should be taken as the model's prognostic temperature
910 in the case of EOS-80 models (since this is the temperature that was used in the
911 bulk formulae), and as the calculated and stored values of potential temperature
912 in the case of TEOS-10 models.

913 Note that this sixth recommendation for EOS-80 based models exposes an unavoidable
914 inconsistency in that the surface values of the model's prognostic temperature is best
915 regarded internally in the ocean model as being Conservative Temperature, but we
916 cannot avoid the fact that this same temperature was used as the sea surface (in situ)
917 temperature in the bulk formulae during the running of such ocean models. Issues such



918 as these would not arise if all ocean models had been converted to the TEOS-10 equation
919 of state.

920 How then should the model's salinity and temperature outputs, S_* and Θ , be used to
921 evaluate dynamical concepts such as streamfunctions etc? The obvious answer that is
922 most consistent with the running of a model is to use the equation of state that the model
923 used, together with the model's temperature and salinity outputs on the native grid of
924 the model. But since we now have the output salinity and temperature of both EOS-80
925 and TEOS-10 models being the same (namely S_* and Θ), there is an efficiency and
926 simplicity argument to analyze the output of all these models in the same manner, using
927 algorithms from the GSW Oceanographic Toolbox (McDougall and Barker, 2011). Doing
928 these model inter-comparisons often involves interpolating the model outputs to
929 different depths (or pressures) than those used in the original ocean model, so incurring
930 some interpolation errors, and while the use of the GSW software means that the in situ
931 density will be calculated slightly differently than in some of the forward models, these
932 differences are small, as can be seen by comparing Figures A.5.1 and A.5.2 of the TEOS-
933 10 Manual, IOC et al. (2010). Hence it seems viable to evaluate density and dynamic
934 height using the GSW Oceanographic Toolbox, with the input salinity to this GSW code
935 being the model's Preformed Salinity, and the temperature input being the Conservative
936 Temperature, which as we have argued, are the model's prognostic variables.

937

938 **Author Contribution**

939 T J McD. devised this new way of interpreting CMIP ocean model variables, P. M. B and
940 R. M. H. provided figures for the paper, and all authors contributed to the concepts and
941 the writing of the manuscript.

942

943 **Acknowledgements.** We have benefitted from helpful comments from Drs. Sjoerd
944 Groeskamp, Fabien Roquet, Geoff Stanley, Casimir de Lavergne, John Krasting and Jan-Erik
945 Tesdal. This paper contributes to the tasks of the Joint SCOR/IAPSO/IAPWS Committee on
946 the Thermophysical Properties of Seawater. T. J. McD, P. M. B and R. M. H gratefully
947 acknowledge Australian Research Council support through grant FL150100090.

948



949 **Appendix A: A non-seawater thermodynamic interpretation of Option 1**

950 Ocean models have always assumed a constant isobaric heat capacity, and have
951 traditionally assumed that the model's temperature variable is whatever temperature
952 the equation of state was designed to accept. Here we enquire whether there is a way of
953 justifying Option 1 thermodynamically in the sense that Option 1 would be totally
954 consistent with thermodynamic principles for a fluid that is different to real seawater.

955 That is, we pursue the idea that these EOS-80 based ocean models are not
956 actually models of seawater, but are models of a slightly different fluid. We require a
957 fluid that is identical to seawater in some respects, such as that it has the same dissolved
958 material (Millero et al., 2008) and the same issues around Absolute Salinity, Preformed
959 Salinity and Practical Salinity, and the same in situ density as real seawater (at given
960 values of Absolute Salinity, potential temperature and pressure). But we require that the
961 expression for the enthalpy of this new fluid is different to that of real seawater.

962 The difference that we envisage between real seawater and this new fluid is that,
963 at zero pressure, the enthalpy of the new fluid is given exactly by the constant value c_p^0
964 times potential temperature θ . That is, for the new fluid, potential enthalpy h^0 is
965 simply $c_p^0\theta$ (as it would be for an ideal gas), and the air-sea interaction for this new fluid
966 would be exactly as it occurs in the EOS-80 based models. Moreover, conservation of
967 potential temperature is justified for this new fluid, and the density and thermal wind
968 would also be correctly evaluated in these EOS-80 based models.

969 The enthalpy of this new fluid is then given by (since $h_p = v$)

$$970 \quad \bar{h}(S_A, \theta, p) = c_p^0 \theta + \int_{p_0}^p \bar{v}(S_A, \theta, p') dp', \quad (\text{A1})$$

971 while the entropy of this new fluid needs to obey the consistency relationship,
972 $\bar{\eta}_\theta = \bar{h}_\theta(p=0)/(T_0 + \theta)$, which reduces to

$$973 \quad \bar{\eta}_\theta = \frac{c_p^0}{(T_0 + \theta)}, \quad (\text{A2})$$

974 where $T_0 = 273.15 \text{ K}$ is the Celsius zero point. This consistency relationship is derived
975 directly from the Fundamental Thermodynamic Relationship (see Table P.1 of IOC et al.,



976 2010). Integrating Eqn. (A2) with respect to potential temperature at constant salinity
977 leads to the following expression for entropy that our new fluid must obey,

$$978 \quad \tilde{\eta}(S_A, \theta) = c_p^0 \ln\left(1 + \frac{\theta}{T_0}\right) + a \left(\frac{S_A}{S_{SO}}\right) \ln\left(\frac{S_A}{S_{SO}}\right). \quad (\text{A3})$$

979 The variation here with salinity is taken from the TEOS-10 Gibbs-function-derived
980 expression for specific entropy which contains the last term in Eqn. (A3) with the
981 coefficient a being $a = -9.310292413479596 \text{ J kg}^{-1} \text{ K}^{-1}$ (this is the value of the coefficient
982 derived from the g_{110} coefficient of the Gibbs function (appendix H of IOC *et al.* (2010)),
983 allowing for our version of the normalization of salinity, (S_A/S_{SO})). This term was
984 derived by Feistel (2008) to be theoretically correct at very small Absolute Salinities.

985 With these definitions, Eqns. (A1) and (A3), of enthalpy and entropy of our new
986 fluid, we have completely defined all the thermophysical properties of the fluid (see
987 Appendix P of IOC *et al.*, 2010 for a discussion). Many aspects of the fluid are different
988 to seawater, including the adiabatic lapse rate (and hence the relationship between in
989 situ and potential temperatures), since the adiabatic lapse rate is given by $\Gamma = \tilde{h}_{\theta p} / \tilde{\eta}_{\theta}$
990 and while the numerator is the same as for seawater (since $\tilde{h}_{\theta p} = \tilde{h}_{\theta p} = \tilde{v}_{\theta}$), the
991 denominator, $\tilde{\eta}_{\theta}$, which is now given by Eqn. (A2), can be up to 6% different to the
992 corresponding function, $\tilde{\eta}_{\theta}$, appropriate to real seawater.

993 We conclude that this is indeed a conceptual way of forcing the EOS-80 based
994 models to be consistent with thermodynamic principles. That is, we have shown that
995 these EOS-80 models are not models of seawater, but they do accurately model a
996 different fluid whose thermodynamic definition we have given in Eqns. (A1) and (A3).
997 This new fluid interacts with the atmosphere in the way that EOS-80 models have
998 assumed to date, the potential temperature of this new fluid is correctly mixed in the
999 ocean in a conservative fashion, and the equation of state is written in terms of the
1000 model's temperature variable, namely potential temperature.

1001 Hence we have constructed a fluid which is different thermodynamically to
1002 seawater, but it does behave exactly as these EOS-80 models treat their model seawater.
1003 That is, we have constructed a new fluid which, if seawater had these thermodynamic
1004 characteristics, then the EOS-80 ocean models would also have correct thermodynamics,



1005 while being able to interpret the model's temperature variable as being potential
1006 temperature.

1007 But this does not change the fact that in order to make these EOS-80 models
1008 thermodynamically consistent in this way we have ignored the real variation at the sea
1009 surface of the isobaric specific heat capacity; a variation that we know can be as large as
1010 6%.

1011 Hence we do not propose this non-seawater explanation as a useful
1012 rationalization of the behaviour of EOS-80 based ocean models. Rather, it seems less
1013 dramatic and more climatically relevant to adopt the simpler interpretation of Option 2.
1014 Under this option we accept that the model is modelling actual seawater, that the
1015 model's temperature variable is in fact Conservative Temperature, and that there are
1016 some errors in the equation of state of these EOS-80 models that amount to errors of the
1017 order of 1% in the thermal wind relation throughout much of the upper (warm) ocean.
1018 That is, so long as we interpret the temperature variable of these EOS-80 based models
1019 as Conservative Temperature, they are fine except that they have used an incorrect
1020 equation of state; they have used $\tilde{\rho}$ rather than $\hat{\rho}$. Apart from this "error" in the ocean
1021 code, Option 2 is a consistent interpretation of the ocean model thermodynamics and
1022 dynamics. In ocean models there are always questions of how to parameterize ocean
1023 mixing. To this uncertain aspect of ocean physics, under Option 2 we add the less than
1024 desirable expression that is used to evaluate density in EOS-80 based ocean models in
1025 CMIP

1026

1027



1028 **Appendix B: An alternative derivation of Eqn. (10)**

1029 Eqn. (10) is an expression for the error in the isobaric density gradient when
 1030 Conservative Temperature is used as the input temperature variable to the EOS-80
 1031 equation of state (which expects its input temperature to be potential temperature). An
 1032 alternative accurate expression to Eqn. (9) for the isobaric density gradient is

$$1033 \quad \tilde{\rho}_{S_*} \nabla_p S_* + \tilde{\rho}_\theta \nabla_p \theta, \quad (B1)$$

1034 and subtracting this from the incorrect expression, Eqn. (8), gives the following
 1035 expression for the model's error in evaluating the isobaric gradient of in situ density,

$$1036 \quad \text{error in } \nabla_p \rho = \tilde{\rho}_\theta \nabla_p (\Theta - \theta). \quad (B2)$$

1037 An approximate fit to the temperature difference, $\Theta - \theta$, as displayed in Figure 2 is

$$1038 \quad (\Theta - \theta) \approx 0.05 \Theta \left(1 - \frac{S_A}{S_{SO}} \right) - 1.75 \times 10^{-3} \Theta \left(1 - \frac{\Theta}{25^\circ\text{C}} \right), \quad (B3)$$

1039 and using this approximate expression in the right-hand side of Eqn. (B2) gives

$$1040 \quad \frac{\text{error in } \nabla_p \rho}{\tilde{\rho}_\theta} \approx \left[0.05 \left(1 - \frac{S_A}{S_{SO}} \right) - 1.75 \times 10^{-3} \left(1 - \frac{\Theta}{12.5^\circ\text{C}} \right) \right] \nabla_p \Theta - \frac{0.05}{S_{SO}} \Theta \nabla_p S_*. \quad (B4)$$

1041 The first part of this expression that multiplies $\nabla_p \Theta$ corresponds to the proportional
 1042 error in the thermal expansion coefficient displayed in Figure 7(a). The second part of
 1043 Eqn. (B4) amounts to an error in the saline derivative of the equation of state, with the
 1044 proportional error (corresponding to Eqn. (12)), being $-0.05 \tilde{\rho}_\theta \Theta / (\hat{\rho}_{S_A} S_{SO})$, and this is
 1045 close to the error that can be seen in Figure 7(b). This error is approximately a quadratic
 1046 function of temperature since the thermal expansion coefficient $\tilde{\rho}_\theta$ is approximately a
 1047 linear function of temperature.

1048

1049

1050



1051
 1052

	Heat flux contributions of different processes	mWm^{-2}
Physical processes	Global warming imbalance (Zanna et al., 2019), mean	+300
	Geothermal heating (Emile-Geay and Madec, 2009), mean	+86
	Viscous dissipation (Graham and McDougall, 2013), mean	+3
	Atmospheric water fluxes of enthalpy (Griffies et al. 2016), mean	- (150-300)
Non-conservation errors	Extra flux of Θ if the air-sea radiative heat flux is taken to occur at a pressure of 25dbar	-0.6
	non-conservation of Θ (Graham & McDougall 2013), mean	+0.3
	non-conservation of Θ (Graham & McDougall 2013), 2*rms	+1
	non-conservation of θ (Graham & McDougall 2013), mean	-10
	non-conservation of θ (Graham & McDougall 2013), 2*rms	± 120
	non-conservation of η (Graham & McDougall 2013), mean	+380
	non-conservation of η (Graham & McDougall 2013), 2*rms	+1200
	Interpreting EOS-80 T as θ (ACCESS-CM2 estimate), mean	+16
Interpreting EOS-80 T as θ (ACCESS-CM2 estimate), 2*rms	± 135	
Numerical errors	ACCESS-OM2 single time-step	$\pm 10^{(-7)}$
	ACCESS-OM2 diagnosed from OHC snapshots	± 0.001
	ACCESS-CM2 diagnosed from OHC monthly-averages	± 0.03

1053
 1054

1055 **Table 1:** Summary of the impact of various processes and modelling errors on the global
 1056 ocean heat budget and its imbalance. All numbers are in units of mWm^{-2} . Numerical errors
 1057 are diagnosed from either ACCESS-OM2 (machine precision errors) or ACCESS-CM2
 1058 (associated with not having access to OHC snapshots). Numbers from interior processes are
 1059 converted to equivalent surface fluxes by depth integration. The sign convention here is that a
 1060 positive heat flux is heat entering the ocean, or warming the ocean by internal dissipation.

1061
 1062



1063 **Code Availability**

1064 This paper has not run any ocean or climate models, and so has not produced any
1065 such computer code. Processed data and code to produce the ACCESS-CM2 figures 5
1066 & 6 is located at the github repository
1067 https://github.com/rmholmes/ACCESS_CM2_SpecificHeat.

1068

1069

1070 **Data Availability**

1071 This paper has not produced any model data. . Processed data and code to produce
1072 the ACCESS-CM2 figures 5 & 6 is located at the github repository
1073 https://github.com/rmholmes/ACCESS_CM2_SpecificHeat.

1074

1075

1076



1077 **References**

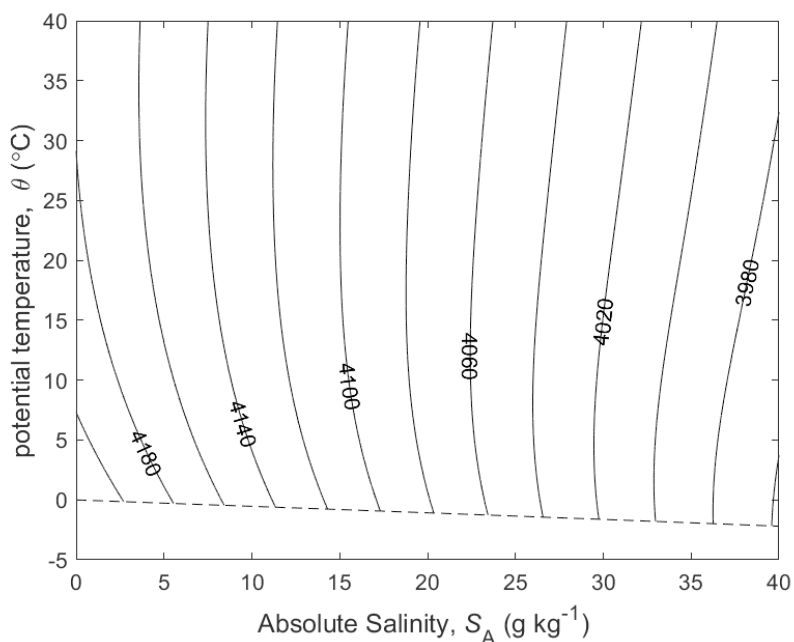
- 1078 Bi, D., Dix, M., Marsland, S., O'Farrell, S., Rashid, H., Uotila, P., Hirst, A., Kowalczyk, E.,
1079 Golebiewski, M., Sullivan, A., Yan, H., Hannah, N., Franklin, C., Sun, Z., Vohralik, P.,
1080 Watterson, I., Zhou, X., Fiedler, R., Collier, M., Ma, Y., Noonan, J., Stevens, L., Uhe, P.,
1081 Zhu, H., Griffies, S., Hill, R., Harris, C. and Puri, K.: The ACCESS coupled model:
1082 description, control climate and evaluation, *Aust. Met. Oceanogr. J.*, **63**, 41-64, 2013.
- 1083 Connors, D. N.: On the enthalpy of seawater. *Limnology and Oceanography*, 15, 587-594,
1084 1970.
- 1085 Cronin M. F., Gentemann C. L., Edson J., Ueki I., Bourassa M., Brown S., Clayson C. A.,
1086 Fairall C. W., Farrar J. T., Gille S. T., Gulev S., Josey S. A., Kato S., Katsumata M., Kent
1087 E., Krug M., Minnett P. J., Parfitt R., Pinker R. T., Stackhouse P. W., Swart S., Tomita H.,
1088 Vandemark D., Weller A. R., Yoneyama K., Yu L., Zhang D.: Air-Sea Fluxes With a
1089 Focus on Heat and Momentum. *Frontiers in Marine Science*, **6**, 430.
1090 <https://www.frontiersin.org/article/10.3389/fmars.2019.00430> , 2019.
- 1091 Emile-Geay J. and Madec G.: Geothermal heating, diapycnal mixing and abyssal circulation.
1092 *Ocean Science*, **5**, 203-217, 2019.
- 1093 Feistel, R.: A Gibbs function for seawater thermodynamics for -6 to 80 °C and salinity up to
1094 120 g kg^{-1} , *Deep-Sea Res. I*, **55**, 1639-1671, 2008.
- 1095 Feistel, R., Wright D. G., Kretzschmar H.-J., Hagen E., Herrmann S. and Span R.:
1096 Thermodynamic properties of sea air. *Ocean Science*, **6**, 91–141. [http://www.ocean-](http://www.ocean-sci.net/6/91/2010/os-6-91-2010.pdf)
1097 [sci.net/6/91/2010/os-6-91-2010.pdf](http://www.ocean-sci.net/6/91/2010/os-6-91-2010.pdf) , 2010.
- 1098 Graham, F. S. and McDougall T. J.: Quantifying the non-conservative production of
1099 Conservative Temperature, potential temperature and entropy. *Journal of Physical*
1100 *Oceanography*, **43**, 838-862. <http://dx.doi.org/10.1175/JPO-D-11-0188.1> , 2013.
- 1101 Griffies, S. M., Danabasoglu, G., Durack, P. J., Adcroft, A. J., Balaji, V., Böning, C. W.,
1102 Chassignet, E. P., Curchitser, E., Deshayes, J., Drange, H., Fox-Kemper, B., Gleckler, P.
1103 J., Gregory, J. M., Haak, H., Hallberg, R. W., Heimbach, P., Hewitt, H. T., Holland, D.
1104 M., Ilyina, T., Jungclaus, J. H., Komuro, Y., Krasting, J. P., Large, W. G., Marsland, S. J.,
1105 Masina, S., McDougall, T. J., Nurser, A. J. G., Orr, J. C., Pirani, A., Qiao, F., Stouffer, R.
1106 J., Taylor, K. E., Treguier, A. M., Tsujino, H., Uotila, P., Valdivieso, M., Wang, Q.,



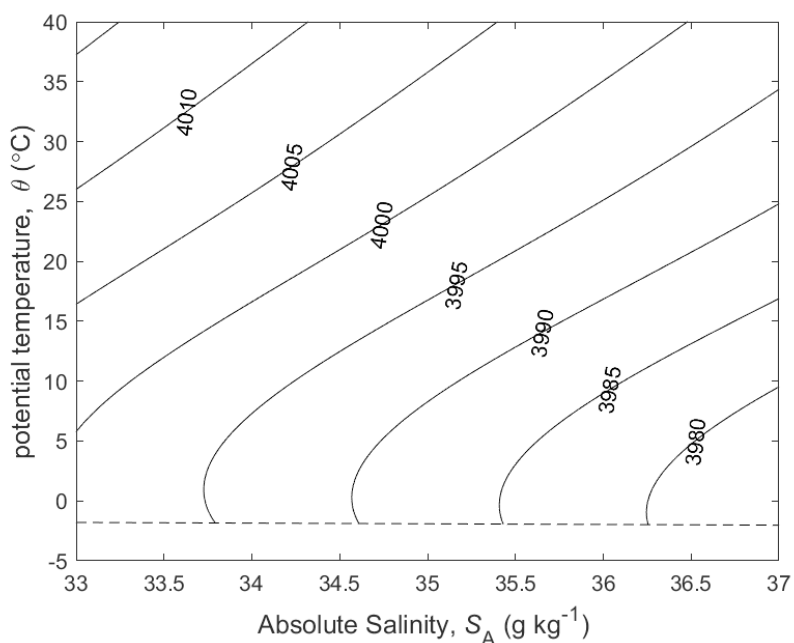
- 1107 Winton, M., and Yeager, S. G.: OMIP contribution to CMIP6: experimental and
1108 diagnostic protocol for the physical component of the Ocean Model Intercomparison
1109 Project. *Geosci. Model Dev.*, **9**, 3231-3296, doi:10.5194/gmd-9-3231-2016.
1110 <http://dx.doi.org/10.5194/gmd-9-3231-2016> , 2016.
- 1111 IOC, SCOR and IAPSO: *The international thermodynamic equation of seawater – 2010:*
1112 *Calculation and use of thermodynamic properties*. Intergovernmental Oceanographic
1113 Commission, Manuals and Guides No. 56, UNESCO (English), 196 pp. available at
1114 http://www.TEOS-10.org/pubs/TEOS-10_Manual.pdf Many of the original papers on
1115 which TEOS-10 is based were published in the following Special Issue of *Ocean Science*,
1116 https://os.copernicus.org/articles/special_issue14.html 2010.
- 1117 Irving, D., Hobbs W., Church J. and Zika J.: A Mass and Energy Conservation Analysis of
1118 Drift in the CMIP6 Ensemble. *Journal of Physical Oceanography*, DOI 10.1175/JCLI-D-
1119 20-0281.1, in press, 2020.
- 1120 Jackett, D. R. and McDougall T. J.: Minimal adjustment of hydrographic profiles to achieve
1121 static stability. *Journal of Atmospheric and Oceanic Technology*, **12**, 381-389.
1122 [https://journals.ametsoc.org/doi/abs/10.1175/1520-](https://journals.ametsoc.org/doi/abs/10.1175/1520-0426%281995%29012%3C0381%3A%20OHPT%3E2.0.CO%3B2)
1123 [0426%281995%29012%3C0381%3A%20OHPT%3E2.0.CO%3B2](https://journals.ametsoc.org/doi/abs/10.1175/1520-0426%281995%29012%3C0381%3A%20OHPT%3E2.0.CO%3B2) , 1995.
- 1124 McCarthy, G.D., Smeed, D.A., Johns, W.E., Frajka-Williams, E., Moat, B.I., Rayner, D.,
1125 Baringer, M.O., Meinen, C.S., Collins, J. and Bryden, H.L.: Measuring the Atlantic
1126 Meridional Overturning Circulation at 26°N. *Progress in Oceanography*, **130**, 91-111.
1127 [doi:10.1016/j.pocean.2014.10.006](https://doi.org/10.1016/j.pocean.2014.10.006) , 2015.
- 1128 McDougall, T. J.: Potential enthalpy: A conservative oceanic variable for evaluating heat
1129 content and heat fluxes. *Journal of Physical Oceanography*, **33**, 945-963.
1130 <https://journals.ametsoc.org/jpo/article/33/5/945/10023/> , 2003.
- 1131 McDougall T. J. and Barker P. M.: *Getting started with TEOS-10 and the Gibbs Seawater*
1132 *(GSW) Oceanographic Toolbox*, 28pp, SCOR/IAPSO WG127, ISBN 978-0-646-55621-5.
1133 available at http://www.TEOS-10.org/pubs/Getting_Started.pdf , 2011.
- 1134 McDougall, T. J. and Feistel R.: What causes the adiabatic lapse rate? *Deep-Sea Research I*,
1135 **50**, 1523-1535. <http://dx.doi.org/10.1016/j.dsr.2003.09.007> , 2003.



- 1136 McDougall, T. J., Jackett D. R., Millero F. J., Pawlowicz R. and Barker P. M.: A global
1137 algorithm for estimating Absolute Salinity. *Ocean Science*, **8**, 1123-1134.
1138 <http://www.ocean-sci.net/8/1123/2012/os-8-1123-2012.pdf> , 2012.
- 1139 Millero, F. J., Feistel R., Wright D. G. and McDougall T. J.: The composition of Standard
1140 Seawater and the definition of the Reference-Composition Salinity Scale. *Deep-Sea*
1141 *Research-I*, **55**, 50-72. <http://dx.doi.org/10.1016/j.dsr.2007.10.001> , 2008.
- 1142 Pawlowicz, R.: A model for predicting changes in the electrical conductivity, Practical Salinity,
1143 and Absolute Salinity of seawater due to variations in relative chemical composition. *Ocean*
1144 *Science*, **6**, 361–378. <http://www.ocean-sci.net/6/361/2010/os-6-361-2010.pdf> , 2010.
- 1145 Pawlowicz, R.: The Absolute Salinity of seawater diluted by riverwater. *Deep-Sea Research I*,
1146 **101**, 71-79, 2015.
- 1147 Pawlowicz, R., Wright D. G. and Millero F. J.: The effects of biogeochemical processes on
1148 oceanic conductivity/salinity/density relationships and the characterization of real seawater.
1149 *Ocean Science*, **7**, 363–387. <http://www.ocean-sci.net/7/363/2011/os-7-363-2011.pdf> , 2011.
- 1150 Pawlowicz, R., McDougall T., Feistel R. and Tailleux R.: An historical perspective on the
1151 development of the Thermodynamic Equation of Seawater – 2010: *Ocean Sci.*, **8**, 161-
1152 174. <http://www.ocean-sci.net/8/161/2012/os-8-161-2012.pdf> , 2012.
- 1153 Roquet, F., Madec G., McDougall T. J. and Barker P. M.: Accurate polynomial expressions for
1154 the density and specific volume of seawater using the TEOS-10 standard. *Ocean*
1155 *Modelling*, **90**, 29-43. <http://dx.doi.org/10.1016/j.ocemod.2015.04.002> , 2015.
- 1156 Tailleux, R.: Observational and energetics constraints on the non-conservation of
1157 potential/Conservative Temperature and implications for ocean modelling. *Ocean*
1158 *Modelling*, **88**, 26-37. <https://doi.org/10.1016/j.ocemod.2015.02.001> , 2015.
- 1159 Wright, D. G., Pawlowicz R., McDougall T. J., Feistel R. and Marion G. M.: Absolute Salinity,
1160 “Density Salinity” and the Reference-Composition Salinity Scale: present and future use
1161 in the seawater standard TEOS-10. *Ocean Sci.*, **7**, 1-26. [http://www.ocean-](http://www.ocean-sci.net/7/1/2011/os-7-1-2011.pdf)
1162 [sci.net/7/1/2011/os-7-1-2011.pdf](http://www.ocean-sci.net/7/1/2011/os-7-1-2011.pdf) , 2011.
- 1163 Zanna L., Khatiwala S., Gregory J. M., Ison, J. and Heimbach P.: Global reconstruction of
1164 historical ocean heat storage and transport, *Proceedings of the National Academy of*
1165 *Sciences*, **116**, 1126-1131, 2019.
- 1166

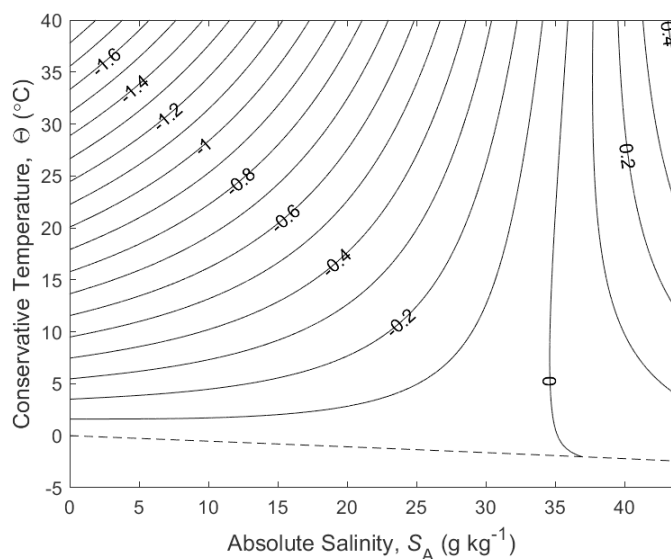


1167

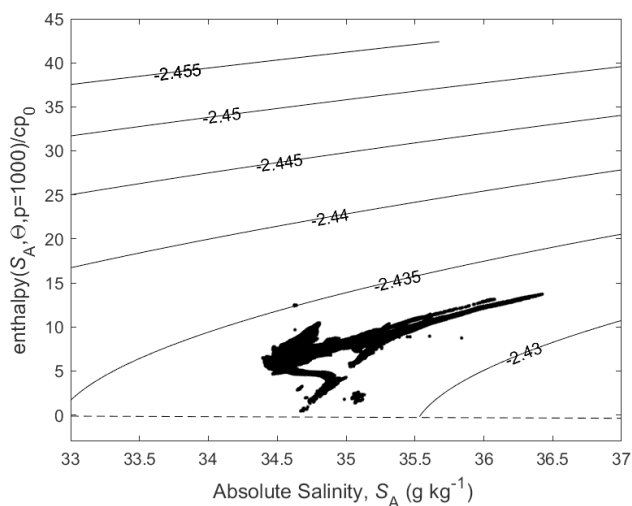


1168
1169
1170
1171
1172

Figure 1. (a) Contours of isobaric specific heat capacity c_p of seawater (in $\text{J kg}^{-1} \text{K}^{-1}$), at $p = 0$ dbar. (b) a zoomed-in version for a smaller range of Absolute Salinity. The dashed line is the freezing line at $p = 0$ dbar.



1173
 1174 **Figure 2.** Contours (in °C) of the difference between potential temperature and
 1175 Conservative Temperature, $\theta - \Theta$.
 1176
 1177



1178
 1179
 1180 **Figure 3.** Contours of $\Theta - \hat{h}(S_A, \Theta, 1000\text{dbar})/c_p^0$ on the Absolute Salinity –
 1181 $\hat{h}(S_A, \Theta, 1000\text{dbar})/c_p^0$ diagram. Enthalpy, $\hat{h}(S_A, \Theta, 1000\text{dbar})$, is a conservative
 1182 quantity for turbulent mixing processes that occur at a pressure of 1000dbar. The
 1183 mean value of the contoured quantity is approximately -2.44°C illustrating that
 1184 enthalpy does not possess the “potential” property; that is, enthalpy increases
 1185 during adiabatic and isohaline increases in pressure. The fact that the contoured
 1186 quantity on this figure is not a linear function of S_A and $\hat{h}(S_A, \Theta, 1000\text{dbar})$
 1187 illustrates the (small) non-conservative nature of Conservative Temperature. The
 1188 dots are data from the world ocean at 1000dbar.
 1189



1190
1191
1192
1193

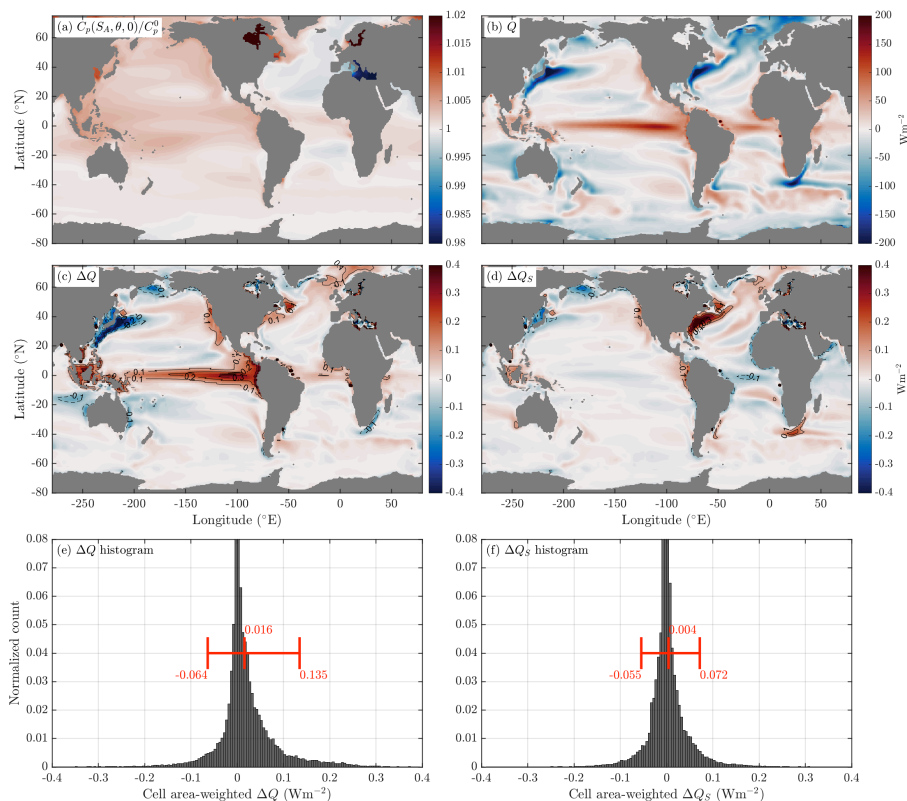


1194
1195
1196
1197
1198
1199
1200
1201
1202
1203

Figure 4. Number line of salinity, illustrating the differences between Preformed Salinity S_* , Reference Salinity S_R , and Absolute Salinity S_A for seawater whose composition differs from that of Standard Seawater which has Reference Composition. If a seawater sample has Reference Composition, then $\delta S_A = 0$ and S_* , S_R and S_A are all equal.



1204



1205
 1206

1207

1208

1209

1210

1211

1212

1213

1214

1215

1216

1217

1218

1219

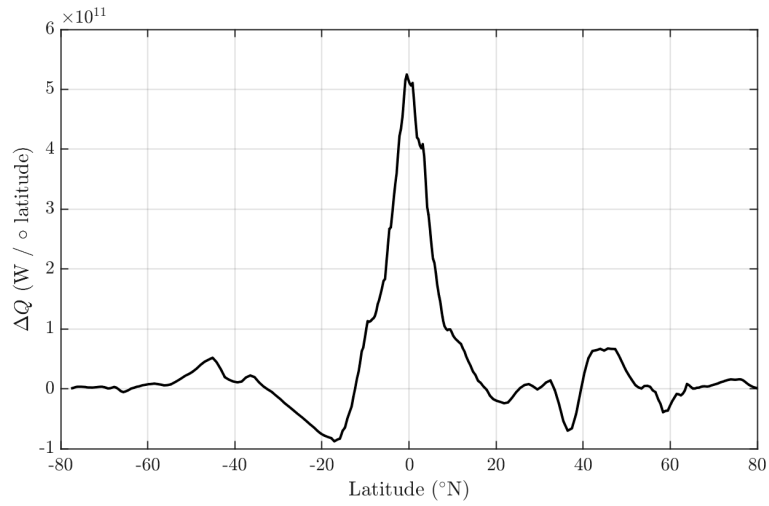
1220

1221

1222

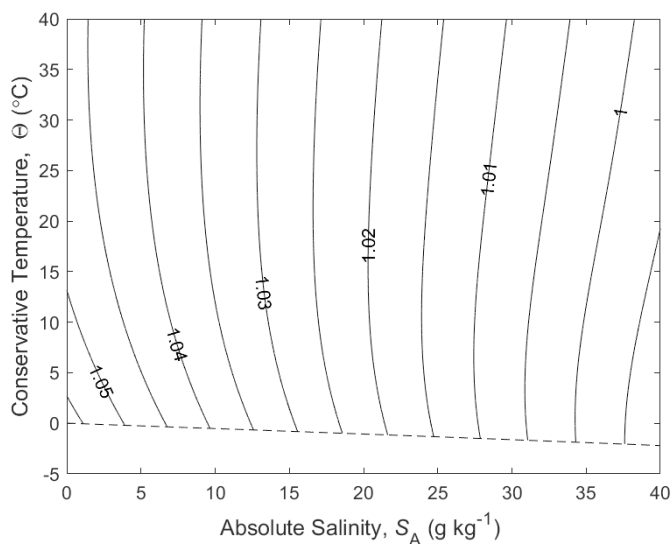
1223

Figure 5. (a) The average value of the ratio of the isobaric specific heat of seawater and c_p^0 for data from the ACCESS-CM2 model's pre-industrial control simulation (600 years long). (b) The average surface heat flux Q (Wm^{-2}) in this same ocean model. (c) The additional heat that the ocean receives/loses compared to the heat that the atmosphere loses/receives (associated with assuming that an EOS-80 model's temperature variable is potential temperature), ΔQ (Wm^{-2} , Eqn. 6). (e) a histogram of ΔQ weighted by the area of each grid cell. (d) The contribution of salinity variations to the air-sea heat flux discrepancy, given by $\Delta Q_s = Q(S - \bar{S})(1/c_p^0) \partial c_p / \partial S$, where \bar{S} is the surface mean salinity and $\partial c_p / \partial S$ is the variation in the specific heat with salinity at the surface mean salinity and potential temperature. (f) a histogram of ΔQ_s weighted by the area of each grid cell. Shown in red in panels e and f are the mean, 5th and 95th percentiles of the histogram (Wm^{-2}). Note that these calculations neglect correlations between surface properties and the surface heat flux at sub-monthly time scales.

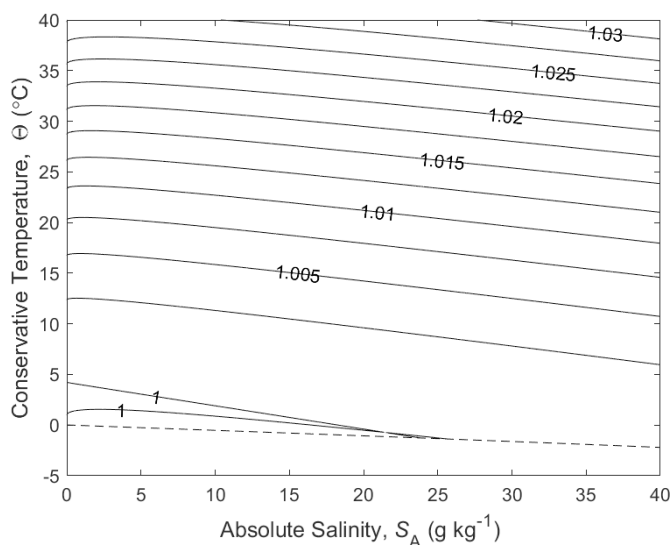


1224
1225
1226
1227
1228
1229

Figure 6. The zonally integrated ΔQ From Fig.5c, showing the imbalance in the air-sea heat flux in Watts per degree of latitude.



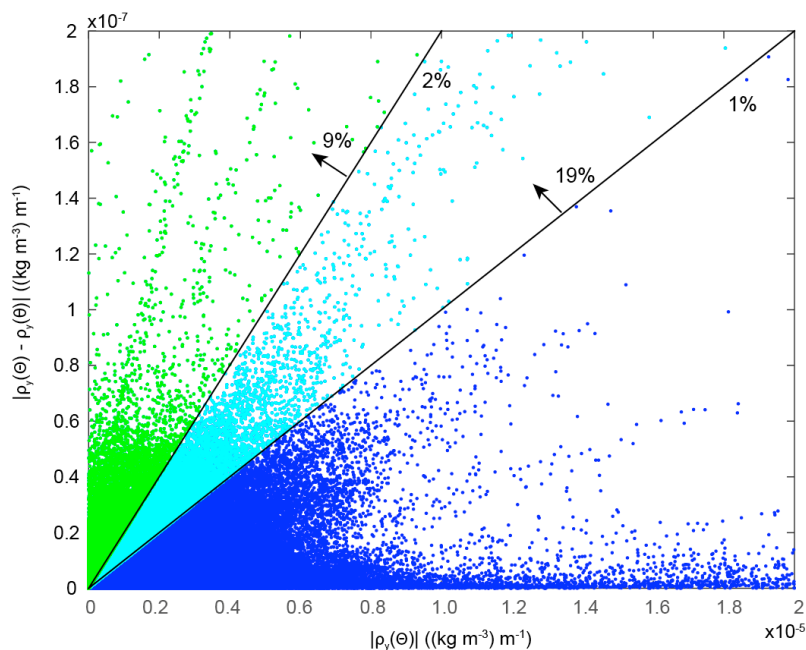
1230



1231
 1232

1233 **Figure 7.** (a) The ratio of the thermal expansion coefficients with respect to Conservative
 1234 Temperature and potential temperature, $\tilde{\alpha}^\theta / \hat{\alpha}^\theta = \tilde{\theta}_\theta$. (b) The ratio of the saline
 1235 contraction coefficients at constant potential temperature to that at constant Conservative
 1236 Temperature, $\hat{\beta}^\theta / \hat{\beta}^\theta = 1 + (\hat{\alpha}^\theta / \hat{\beta}^\theta) \hat{\theta}_{S_A} / \hat{\theta}_\theta$ at $p = 0$ dbar.

1237
 1238



1239

1240 **Figure 8.** The northward density gradient at constant pressure (the horizontal axis) for
1241 data in the global ocean atlas of Gouretski and Koltermann (2004) for $p < 1000$ dbar. The
1242 vertical axis is the magnitude of the difference between evaluating the density gradient
1243 using Θ versus θ as the temperature argument in the expression for density. This is
1244 virtually equivalent to the density difference between calling the EOS-80 and the TEOS-10
1245 equations of state, using the same numeric inputs for each. The 1% and 2% lines indicate
1246 where the isobaric density gradient is in error by 1% and 2%. 19% of the data shallower
1247 than 1000 dbar has the isobaric density gradient changed by more than 1% when
1248 switching between the equations of state. The median value of the percentage error in the
1249 isobaric density gradient is 0.22%.

1250

1251